lower case

New Constraints on $\Omega_{\rm M}$ and Ω_Λ From an Independent Set of High-Redshift Supernovae Observed With HST[1]

Version 2003-Apr-30

R. A. Knop[2,3,4], G. Aldering[5,4], R. Amanullah[6], P. Astier[7], K. Barton[8], G. Blanc[5], M. S. Burns[8], A. Conley[5,9], S. E. Deustua[5,10], M. Doi[11], R. Ellis[12], S. Fabbro[13,4], G. Folatelli[6], A. S. Fruchter[14], G. Garavini[6], S. Garmond[5,9], R. Gibbons[5], G. Goldhaber[5,9], A. Goobar[6], D. E. Groom[5,4], D. Hardin[7], I. Hook[15], D. A. Howell[5], M. Irwin[16], A. G. Kim[5,4], B. C. Lee[5], C. Lidman[17], R. McMahon[16], J. Mendez[18,19], S. Nobili[6], P. E. Nugent[5,4], R. Pain[7], N. Panagia[14], C. R. Pennypacker[5], S. Perlmutter[5], V. Prasad[5], R. Quimby[5], J. Raux[7], N. Regnault[5], P. Ruiz-Lapuente[19], G. Sainton[7], B. Schaefer[20], K. Schahmaneche[7], E. Smith[2], A. L. Spadafora[5], V. Stanishev[6], M. Sullivan[21,12], N. A. Walton[16], L. Wang[5], W. M. Wood-Vasey[5,9], and N. Yasuda[22] (THE SUPERNOVA COSMOLOGY PROJECT)

ABSTRACT

This paper presents measurements of $\Omega_{\rm M}$ and Ω_Λ from 11 supernovae with high-quality lightcurves measured ~~with~~ using WFPC2 on the HST. This is an independent set of high-redshift supernovae that confirm previous supernova evidence for an accelerating Universe. Because of the high-quality lightcurves available from photometry on WFPC2, these 11 supernovae alone provide limits on the cosmological parameters comparable in statistical weight to the previous results. Combined with earlier Supernova Cosmology Project data, the new supernovae yield a measurement of the mass density $\Omega_{\rm M} = 0.21^{+0.06}_{0.05}$ (statistical) ± 0.04 (identified systematics), or equivalently a cosmological constant of $\Omega_\Lambda = 0.79^{+0.05}_{0.06}$ (statistical) ± 0.04 (identified systematics), under the assumption of a flat universe. When the supernova results are combined with ~~an~~ independent flat-universe measurements of $\Omega_{\rm M}$ from CMB and large scale structure data, they provide a value for the dark energy equation of state parameter of $w = \quad 1.15^{+0.17} \quad 0.22$ (statistical) $\pm \sim 0.05$ (identified systematic), if w is assumed to be constant in time. In addition to high-precision lightcurve measurements, the new data offer greatly improved color measurements of the high-redshift supernovae, and hence host-galaxy $E(B\text{-}V)$ estimates. These measurements indicate that only one ~~or two~~ of the 11 new supernovae suffers significant host-galaxy extinction; there is no trend of anomalous $E(B\text{-}V)$ at higher redshifts. The precision of the measurements is such that it is possible to perform a host-galaxy extinction correction directly to individual supernovae without any assumptions or priors on the $E(B\text{-}V)$ distribution, yielding results consistent with current and previous results; host-galaxy reddening is not a source of systematic uncertainty ~~which~~ that can explain the luminosity distance of high-redshift supernovae without recourse to an accelerating expansion.

wording confusing

[1]Based in part on observations made with the NASA/ESA Hubble Space Telescope, obtained at the Space Telescope Science Institute, which is operated by the Association of Universities for Research in Astronomy, Inc., under NASA contract NAS 5-26555. These observations are associated with programs #7336, #7590, and #8346.

Don't forget to spell check.

lower case

1. Introduction

In a series of papers culminating in 1998, two teams reported observations of Type Ia Supernovae (SNe Ia), which gave strong evidence for an acceleration of the Universe's expansion, and hence for a non-zero cosmological constant, or dark energy density (Perlmutter *et al.* 1998; Garnavich *et al.* 1998a; Schmidt *et al.* 1998; Riess 1998; Perlmutter *et al.* 1999). These results ruled out a flat, matter-dominated ($\Omega_{\rm M} = 1$, $\Omega_\Lambda = 0$) universe. For a flat universe, motivated by inflation theory, they yielded a value for the cosmological constant of $\Omega_\Lambda \simeq 0.7$. Even in the absence of assumptions about the geometry of the Universe, the supernova results indicate at greater than 99% confidence the existence of a cosmological constant. (For a review, see Perlmutter & Schmidt 2003.)

The supernova results combined with observations of the power spectrum of the Cosmic Microwave Background (CMB) (e.g., Jaffe *et al.* 2001) and the density of massive clusters (e.g., Turner 2001; Allen, Schmidt, & Fabian 2002; Bahcall *et al.* 2003) from dynamical redshift-space distortions (Hawkins *et al.* 2002) yield a consistent picture of a flat universe with $\Omega_{\rm M} \simeq 0.3$ and $\Omega_\Lambda \simeq 0.7$ (Bahcall *et al.* 1999). Each of these measurements are sensitive to different linear combinations of the parameters, and hence they complement each other. Moreover, because there are three different measurements of two parameters, the combination provides an important consistency check. While the current observations of massive clusters and high-redshift supernovae primarily probe the "recent" Universe at redshifts of $z < 1$, the CMB measurements probe the early Universe at $z \sim 1100$. That consistent results are obtained by measurements of vastly different epochs of the Universe's history is a vindication of the standard model of the expanding Universe.

Need more CMB refs. Get from Martin White (or maybe Eric Linder).

In the redshift range around $z = 0.4$–0.7, the supernova results are most sensitive to a linear combination of $\Omega_{\rm M}$ and Ω_Λ close to $\Omega_{\rm M} \quad \Omega_\Lambda$. In contrast, clusters are sensitive primarily to $\Omega_{\rm M}$ alone, while the CMB is most sensitive to $\Omega_{\rm M}+\Omega_\Lambda$.

Some of the data presented herein were obtained at the W.M. Keck Observatory, which is operated as a scientific partnership among the California Institute of Technology, the University of California and the National Aeronautics and Space Administration. The Observatory was made possible by the generous financial support of the W.M. Keck Foundation. Based in part on observations obtained at the WIYN Observatory, which is a joint facility of the University of Wisconsin-Madison, Indiana University, Yale University, and the National Optical Astronomy Observatory. Based in part on observations made with the European Southern Observatory telescopes (ESO programmes 60.A-0586 and 265.A-5721)

[2]Department of Physics and Astronomy, Vanderbilt University, Nashville, TN 37240, USA

[3]Visiting Astronomer, Kitt Peak National Observatory, National Optical Astronomy Observatory, which is operated by the Association of Universities for Research in Astronomy, Inc. (AURA) under cooperative agreement with the National Science Foundation.

[4]Visiting Astronomer, Cerro Tololo Interamerican Observatory, National Optical Astronomy Observatory, which is operated by the Association of Universities for Research in Astronomy, Inc. (AURA) under cooperative agreement with the National Science Foundation.

[5]E. O. Lawrence Berkeley National Laboratory, 1 Cyclotron Rd., Berkeley, CA 94720, USA

[6]Department of Physics, Stockholm University, SCFAB, S-106 91 Stockholm, Sweden

[7]LPNHE, CNRS-IN2P3, University of Paris VI & VII, Paris, France

[8]Colorado College 14 East Cache La Poudre St., Colorado Springs, CO 80903

[9]Department of Physics, University of California Berkeley, Berkeley, 94720-7300 CA, USA

[10]American Astronomical Society, 2000 Florida Ave, NW, Suite 400, Washington, DC, 20009 USA.

[11]Department of Astronomy and Research Center for the Early Universe, School of Science, University of Tokyo, Tokyo 113-0033, Japan

[12]California Institute of Technology, E. California Blvd, Pasadena, CA 91125, USA

[13]IST, Lisbon, Portugal

[14]Space Telescope Science Institute, 3700 San Martin Drive, Baltimore, MD 21218, USA

[15]Department of Physics, University of Oxford, Nuclear & Astrophysics Laboratory Keble Road, Oxford, OX1 3RH, UK

[16]Institute of Astronomy, Madingley Road, Cambridge CB3 0HA, UK

[17]European Southern Observatory, Alonso de C ordova 3107, Vitacura, Casilla 19001, Santiago 19, Chile

[18]Isaac Newton Group, Apartado de Correos 321, 38780 Santa Cruz de La Palma, Islas Canarias, Spain

[19]Department of Astronomy, University of Barcelona, Barcelona, Spain

[20]University of Texas, Department of Astronomy, C-1400, Austin, TX,78712, U.S.A.

[21]Department of Physics, University of Durham, South Road, Durham, DH1 3LE, UK

[22]National Astronomical Observatory, Mitaka, Tokyo 181-8588, Japan

Add a new short paragraph here summarizing what we found in Sullivan et al (2002). This should be written to make it clear that this Sullivan et al paper was the first major new result paper to kick off the next round of results after the 1998 discoveries -- and it came from us (SCP).

Of the three cosmological measurements, the supernovae taken alone thus provide the best *direct* evidence for dark energy; even under the assumption of a flat universe, it is the supernovae that indicate the presence of dark energy. Therefore, it is of importance to improve the precision of the result, to confirm the result with additional independent high-redshift supernovae, and also to limit the possible effects of systematic errors.

This paper presents 11 new supernovae discovered and observed by the Supernova Cosmology Project (SCP) at redshifts $0.35 < z < 0.86$, a range very similar to that of the 42 high-redshift supernovae reported in Perlmutter *et al.* (1999, hereafter P99). The supernovae of that paper, with one exception, were observed entirely with ground-based telescopes; the 11 supernovae of this work have complete lightcurves in both the R and I bands measured with the Wide-Field/Planetary Camera (WPFC2) on the Hubble Space Telescope (HST). The HST provides two primary advantages for photometry of point sources such as supernovae. First, from orbit, the sky background is much lower, allowing a much higher signal-to-noise ratio in a single exposure. Second, because the telescope is not limited by atmospheric seeing, it has very high spatial resolution. This helps the signal-to-noise ratio by greatly reducing the area of background emission which contributes to the noise of the source measurement, and moreover simplifies the task of separating the variable supernova signal from the host galaxy. With these advantages, the precision of the lightcurve and color measurements is ~~so~~ much greater for the 11 supernovae in this paper than was possible with previous ground-based observations. These 11 supernovae themselves provide a high-precision *new* set of supernovae to test the accelerating universe results.

nsert: leven [[check this umber]] of he 14 new Ne reported n Riess et al 1998) were lso bserved rom the round.

Perlmutter *et al.* (1997, 1999) and Riess (1998) presented extensive accounts of, and bounds for, possible systematic uncertainties in the supernova measurements. One obvious possible source of systematic uncertainty that was discussed is the effect of host galaxy dust. For a given mass density, the effect of a cosmological constant on the magnitudes of high-redshift supernovae is to make their observed brightness *dimmer* than would have been the case with $\Omega_\Lambda = 0$. Dust extinction from within the host galaxy of the high-redshift supernovae could have a similar effect; however, dust extinction will also tend to redden the colors of the supernovae. Therefore, a measurement of the color of the high-redshift supernovae, compared to the known colors of SNe Ia, has been used to provide an a upper limit on the effect of host-galaxy dust extinction, or a direct measurement of that extinction which may then be corrected. These color measurements' uncertainties usually dominate the statistical error of photometric measurements. Previous analyses have either selected a low-extinction subset of high-redshift supernovae and not applied corrections directly Fit C of (P99), or have used a biasing Bayesian prior on the intrinsic extinction distribution to limit the propagated uncertainties of errors in color measurements (Fit E of P99, Riess 1998). The much higher precision of the HST lightcurves of this paper allow us to make high-quality, unbiased, individual host-galaxy extinction corrections to each supernova event.

In this paper, we first describe the PSF-fit photometry method used for extracting the lightcurves from the WPFC2 images. Next, we describe the lightcurve fitting procedure, including the methods used for calculating accurate K-corrections. So that all supernovae may be treated consistently, we apply the slightly updated K-correction procedure to all of the supernovae used in P99. We discuss the evidence for host-galaxy extinction (only significant for one of the 11 new supernovae) from the R-I lightcurve colors. We present the limits on the cosmological parameters Ω_M and Ω_Λ from the new dataset alone as well as combining this data set with the data of P99; this latter fit provides the best current limit on cosmological parameters from high-redshift SNe Ia. Finally, we present the limits on w, the equation of state of the dark energy, from these data, and from these data combined with recent CMB and galaxy two-point correlation results. Updated analyses of systematic uncertainties are presented for these measurements.

2. Observations, Data Reduction, and Analysis

2.1. WFPC2 Photometry

The supernovae discussed in this paper are listed in Table 1. They were discovered during three different supernova searches following the techniques described in Perlmutter *et al.* (1995, 1997, 1999). Two of the searches were conducted at the 4m Blanco telescope at the Cerro Tololo Inter-American Observatory (CTIO), in December 1997 and March/April 1998. The final search was conducted at the Canada-France-Hawaii Telescope (CFHT) on Mauna Kea in Hawaii in April/May 2000. In each case, 2–3 nights of reference images were followed 3–4 weeks later by 2–3 nights of search images. The two images of each search field were seeing-matched and subtracted, and were searched for residuals indicating a supernova candidate. The March/April 1998 search originally targeted primarily higher-redshift supernovae to be observed by the HST, but marginal weather conditions limited the depth of the search. As a result, the 11 HST supernovae reported in this paper are at spaced approximately evenly in the range $0.3 < z < 0.8$.

I still think this should be cut. (At the very least, it should just excuse one or two of the lowest z SNe.)

[Move footnote number]

Spectra were obtained ~~at~~ with the red-~~side of~~ arm LRIS (Oke *et al.* 1995) on the Keck 10m telescope, with FORS1 on Antu (VLT-UT1) (Appenzeller *et al.* 1998), ~~and with WFOSC2~~ on the ESO 3.6m telescope.[23] These spectra were used to confirm the identification of the candidates as SNe Ia, and to measure the redshift of each candidate. All eleven supernovae in the set have strong confirmation as type Ia, although there is no measurement of the Si II λ6150 feature (Pskovskii 1969; Branch & Patchet 1973) for the higher redshift supernovae (SNe 1997ek, 1997ez, 1998ay, 1998be, and 1998bi). For these all were identified as being of Type Ia based on the presence of Si II at λ4190.7 or by the fact that the Fe II features in the spectra matched those of Type Ia's at a similar lightcurve epoch. Sne Ib/c near maximum light are easily distinguished from SNe Ia by the fact that they never show Si II at λ4190.7, and the Fe II features in their spectra are more similar to SNe Ia at two weeks after peak brightness (Nugent 2003).

Where possible, the redshift z of each candidate was measured by matching narrow features in the host galaxy of the supernovae; the precision of these measurements in z is typically 0.001. In cases where there were not sufficient host galaxy features (SN 1998aw and SN 1998ba), redshifts were measured from the supernova itself; in these cases, z is ~~precise (conservatively) to~~ measured with a (conservative) precision of 0.01

[23]http://www.ls.eso.org/lasilla/sciops/efosc/

(Branch & van den Bergh 1993). Even in the latter case redshift measurements do not contribute significantly to the uncertainties in the final cosmological measurements since these are dominated by the photometric uncertainties.

Each of these supernovae was followed with two broadband filters with the Wide Field/Planetary Camera 2 (WFPC2) on the Hubble Space Telescope (HST). Table 1 lists the dates of these observations. The two filters were chosen to have ~~be those with~~ maximum sensitivity to these faint objects, while being ~~and which were~~ as close a match as practical to the rest-frame B and V filters at the targeted redshifts. At the redshifts for the supernovae in this paper, the filters used approximate the ground-based R-band (F675W) and I-band (F814W) filters ~~(with~~ based on the effective system transmission curves provided by the Space Telescope Science Institute). These filters roughly correspond to redshifted B- and V-band filters for the supernovae at $z < 0.7$, and redshifted U- and B- band filters for the supernovae at $z > 0.7$.

Supernovae were imaged with the Planetary Camera (PC) chip of WFPC2, which has a scale of 0.046″/pixel. The HST images were reduced through the standard HST "On-The-Fly Reprocessing" data reduction pipeline provided by the Space Telescope Science Institute. Images were background subtracted, and images taken in the same orbit were combined to reject cosmic rays using the "crrej" procedure (a part of the STSDAS IRAF package). Photometric fluxes were extracted from the final images using a PSF-fitting procedure. Traditional PSF fitting procedures assume a single isolated point source above a constant background. In this case, the point source was superimposed on top of the image of the host galaxy. In all cases, the supernova image was separated from the core of the host galaxy; however, in most cases the separation was not enough that an annular measurement of the background would be accurate. Because the host galaxy flux should be constant in all of the images, we used a PSF fitting procedure that ~~which~~ fit a PSF *simultaneously* to every image of a given supernovae observed through a given photometric filter. The model we fit was:

$$f_i(x,y) = f_{0i} \times \mathrm{psf}(x \quad x_{0i}, y \quad y_{0i}) + \mathrm{bg}(x \quad x_{0i}, y \quad y_{0i}; a_j) + p_i \qquad (1)$$

Table 1: WFPC2 Supernova Observations

SN Name	z	F675W Observations	F814W Observations
1997ek	0.863	1998-01-05 (400s,400s)	1998-01-05 (500s,700s)
		1998-01-11 (400s,400s)	1998-01-11 (500s,700s)
			1998-02-02 (1100s,1200s)
			1998-02-14 (1100s,1200s)
			1998-02-27 (1100s,1200s)
			1998-11-09 (1100s,1300s)
			1998-11-16 (1100s,1300s)
1997eq	0.538	1998-01-06 (300s,300s)	1998-01-06 (300s,300s)
		1998-01-21 (400s,400s)	1998-01-11 (300s,300s)
			1998-02-02 (500s,700s)
		1998-02-11 (400s,400s)	1998-02-11 (500s,700s)
		1998-02-19 (400s,400s)	1998-02-19 (500s,700s)
1997ez	0.778	1998-01-05 (400s,400s)	1998-01-05 (500s,700s)
		1998-01-11 (400s,400s)	1998-01-11 (500s,700s)
			1998-02-02 (1100s,1200s)
			1998-02-14 (1100s,1200s)
			1998-02-27 (100s,1200s,1100s,1200s)
1998as	0.355	1998-04-08 (400s,400s)	1998-04-08 (500s,700s)
		1998-04-20 (400s,400s)	1998-04-20 (500s,700s)
		1998-05-11 (400s,400s)	1998-05-11 (500s,700s)
		1998-05-15 (400s,400s)	1998-05-15 (500s,700s)
		1998-05-29 (400s,400s)	1998-05-29 (500s,700s)
1998aw	0.440	1998-04-08 (300s,300s)	1998-04-08 (300s,300s)
		1998-04-18 (300s,300s)	1998-04-18 (300s,300s)
		1998-04-29 (400s,400s)	1998-04-29 (500s,700s)
		1998-05-14 (400s,400s)	1998-05-14 (500s,700s)
		1998-05-28 (400s,400s)	1998-05-28 (500s,700s)
1998ax	0.497	1998-04-08 (300s,300s)	1998-04-08 (300s,300s)
		1998-04-18 (300s,300s)	1998-04-18 (300s,300s)
		1998-04-29 (300s,300s)	1998-04-29 (500s,700s)
		1998-05-14 (300s,300s)	1998-05-14 (500s,700s)
		1998-05-27 (300s,300s)	1998-05-27 (500s,700s)
1998ay	0.638	1998-04-08 (400s,400s)	1998-04-08 (500s,700s)
		1998-04-20 (400s,400s)	1998-04-20 (500s,700s)
			1998-05-11 (1100s,1200s)
			1998-05-15 (1100s,1200s)
			1998-06-03 (1100s,1200s)
1998ba	0.430	1998-04-08 (300s,300s)	1998-04-08 (300s,300s)
		1998-04-19 (300s,300s)	1998-04-19 (300s,300s)
		1998-04-29 (400s,400s)	1998-04-29 (500s,700s)
		1998-05-13 (400s,400s)	1998-05-13 (500s,700s)
		1998-05-28 (400s,400s)	1998-05-28 (500s,700s)
1998be	0.644	1998-04-08 (300s,300s)	1998-04-08 (300s,300s)
		1998-04-19 (300s,300s)	1998-04-19 (300s,300s)
		1998-04-30 (400s,400s)	1998-04-30 (500s,700s)
		1998-05-15 (400s,400s)	1998-05-15 (500s,700s)
		1998-05-28 (400s,400s)	1998-05-28 (500s,700s)
1998bi	0.740	1998-04-06 (400s,400s)	1998-04-06 (500s,700s)
		1998-04-18 (400s,400s)	1998-04-18 (500s,700s)
			1998-04-28 (1100s,1200s)
			1998-05-12 (1100s,1200s)
			1998-06-02 (1100s,1200s)
2000fr	0.543		2000-05-08 (2200s)
		2000-05-15 (600s,600s)	2000-05-15 (1100s,1100s)
		2000-05-28 (600s,600s)	2000-05-28 (600s,600s)
		2000-06-10 (500s,500s)	2000-06-10 (600s,600s)
		2000-06-22 (1100s,1300s)	2000-06-22 (1100s,1200s)
		2000-07-08 (1100s,1300s)	2000-07-08 (110s,1200s)

where $f_i(x, y)$ is the measured flux in pixel (x, y) of the ith image, (x_{0i}, y_{0i}) is the position of the supernova on the ith image, f_{0i} is the total flux in the supernova in the ith image, $\mathrm{psf}(u, v)$ is a normalized point spread function, $\mathrm{bg}(u, v)$ is a constant background parametrized by a_j, and p_i is a pedestal offset for the ith image. There are $4n + m$ 1 parameters in this model, where n is the number of images (typically 2, 5, or 6 summed images) and m is the number of parameters a_j that specifies the background model (typically 3 or 6). (The 1 is due to the fact that a zeroth-order term in the background is degenerate with one of the p_i terms.) Parameters varied include f_i, x_{0i}, y_{0i}, p_i, and a_j.

[Start new paragraph here.]]

Due to the scarcity of objects in our images, geometric transformations between the images at different epochs using other objects on the four chips of WFPC2 allowed an *a priori* determination of (x_{0i}, y_{0i}) good to only ~ 1 pixel. Allowing those parameters to vary in the fit (effectively, using the point source signature of the supernova to determine the offset of the image) provided position measurements a factor of ~ 10 better.

Pushing center of PSF fit towards brighter pixels will bias the fit, won't it? Or do you know that the covariance is small between position and flux amplitude fit.

The model was fit to 7×7 or 9×9 pixel patches extracted from all of the images of a time sequence of a single supernova in a single filter. The series of f_{0i} values, corrected as described in the rest of this section, provided the data used in the lightcurve fits described in § 2.2. For one supernova (SN 1997ek) the F814W background was further constrained by a supernova-free "final reference" image taken 11 months after the supernova explosion. (Although obtaining final references to subtract the galaxy background is standard procedure for ground-based photometry of high-redshift supernovae, the higher resolution of WFPC2 provides sufficient separation between the supernova and host galaxy that such images are not always necessary, particularly in this redshift range.)

Add this missing close parenthesis]

A single Tiny Tim PSF (Krist & Hook 2001), corrected by an empirical electron diffusion term (Fruchter 2000), was used as $\mathrm{psf}(u, v)$ for all images of a given band. Although this is an approximation– the PSF of WFPC2 depends on the epoch of the observation as well as the position on the chip– this approximation should be a good one, especially given that for all of the observations the supernova was positioned close to the center of the PC. To verify that this approximation is valid, we reran the PSF fitting procedure with individually generated PSFs for most supernovae. The measured fluxes were not significantly different, showing differences in both directions generally within 1–2% of the supernova peak flux value, much less than our photometric uncertainties on individual data points.

One of the great advantages of the Hubble Space Telescope is its low background. However, CCD photometry of faint objects over a low background suffers from an imperfect charge transfer efficiency (CTE) effect, which can lead to a systematic underestimate of the flux of point sources. On the PC, these effects can be as large as $\sim 15\%$. The measured flux values (f_i above) extracted were corrected for the CTE of WFPC2 following the standard procedure of Dolphin (2000).[24] Because the host galaxy is a smooth background underneath the point source, it was considered as a contribution to the background in the CTE correction. For an image which was a combination of several separate exposures within the same orbit or orbits, the CTE calculation was performed assuming that each SN image had a measured flux whose fraction of the total SN flux was equal to the fraction of that individual image's exposure time to the summed image's total exposure time.

[[This is correct isn't it -- that you mean *SN* image and flux?]]

In addition to the HST data, there exists some ground-based photometry for each of these SNe. This includes the images from the search itself, as well as a limited amount of follow-up. The details of which supernovae were observed with which telescopes are given with the lightcurves in Appendix A. Ground-based photometric fluxes were extracted from images using the same aperture photometry procedure of P99. A complete lightcurve in a given filter (R or I) combined the HST data with the ground-based data (using the color correction procedure described below in § 2.3), using measured zeropoints for the ground-based data and the Vega zeropoints of Dolphin (2000) for the HST data. The uncertainties on those zeropoints (0.003 for F814W or 0.006 for F675W) were added as correlated errors between all HST data points when combining with the ground-based lightcurve. Similarly, the measured uncertainty in the ground-based zeropoint

[24] ~~Updated by the coefficients posted later on the author's web page in May, 2001.~~

These CTE corrections used updated coefficients posted later on Dophin's web page (http:// xxx.xxx.xxx) in May 2001.

was added as a correlated error to all ground-based fluxes.

2.2. Lightcurve Fits

It is the magnitude of the supernova at its lightcurve peak that serves as a ~~standard~~ "calibrated" candle in estimating the cosmological parameters from the luminosity distance relationship. To estimate this peak magnitude, we performed template fits to the time series of photometric data for each supernova. In addition to the 11 SNe described here, lightcurve fits were also performed to the supernovae from P99, including 18 supernovae from Hamuy *et al.* (1996, hereafter H96), and eight from Riess (1999a, hereafter R99) which match the same selection criteria used for the H96 supernovae (having data within six days of maximum light and located at $cz > 4000$ km/s) i.e., in the Hubble flow. Because of new templates and K-corrections (see below), lightcurve fits to the photometric data on the 42 high-redshift ~~of~~ supernovae of P99 were redone for this paper for consistency.

Lightcurve fits were performed using a χ^2-minimization procedure based on MINUIT (James & Roos 1975). For both high and low-redshift supernovae, color corrections and K-corrections are applied (see § 2.3) to the photometric data. These data were then fit to lightcurve templates. Fits were performed to the combined R and I band data for each high-redshift supernova. (The exceptions are the seven high-redshift supernovae from P99 for which no I-band lightcurve is available, and which are therefore not included in the main analyses of this paper.)

Are these 7 SNe ever used in this paper? If not, delete this parenthetical sentence, and also remove from Table, except to add a footnote to the table saying they have been cut out and why.

For low-redshift supernovae, fits were performed using only the B and V band data (which correspond to de-redshifted R and I bands for most of the high-redshift supernovae). The lightcurve model fit to the supernova has four parameters to modify the lightcurve templates: time of rest-frame B-band maximum light, peak flux in R, R-I color, and stretch s. Stretch (Perlmutter *et al.* 1997; Goldhaber *et al.* 2001) is a parameter which linearly scales the time axis ~~relative to maximum light~~, so that a supernova with a high stretch has a relatively slow decay from maximum, and a supernova with a low stretch has a relatively fast decay from maximum. For supernovae in the redshift range $z = 0.3$–0.7, a B template was fit to the R-band lightcurve and a V template was fit to the I-band lightcurve. For supernovae at $z > 0.7$, a U template was fit to the R-band lightcurve and a B template to the I-band lightcurve. Two of the high redshift supernovae from P99 fall at $z \sim 0.18$ (SN 1997I and SN 1997N); for these supernovae, V and R templates were fit to the R and I band data. (The peak B band magnitude was extracted by adding the intrinsic SN Ia B-V color to the fit V band magnitude at the epoch of B maximum.)

The B template used in the lightcurve fits was that of Goldhaber *et al.* (2001). For this paper, new V-band and R-band templates were generated following a procedure similar to that of Goldhaber *et al.* (2001), by fitting a smooth parametrized curve through the low-z supernova data of H96 and R99. A new U-band template was generated with data from Hamuy *et al.* (1991), Lira *et al.* (1998), Richmond *et al.* (1995), Suntzeff *et al.* (1999), and Wells *et al.* (1994). This template also fits very well [Quantify, Ariel] to the U-band data of Jha (2002). Each of these new templates was fit to the low-redshift supernova data simultaneously with a stretch fit of the B-template to the B-band data of the same supernova, thereby guaranteeing that the fit templates correspond to a stretch=1 supernova.

Re-word: confusing

Lightcurve templates had an initial parabola with a 20-day rise time (Aldering, Knop, & Nugent 2000), joined to a smooth spline section to describe the main part of the lightcurve, then joined to an exponential decay to describe the final tail at $>\sim 70$ days past maximum light. The first 90 days of each of the three templates is shown in Table 2. Due to a secondary "hump" or "shoulder" ~ 20 days after maximum, the R-band lightcurve does not ~~appear to~~ vary strictly according to the single simple stretch parameter which is so successful in describing the different U-, B-, and V-band lightcurves. However, for the two supernovae at z ~ 0.18, the peak R and I band magnitudes are very well constrained, and the stretch is also well-measured from the R band (rest frame V band) lightcurve.

Nonetheless, the lightcurve fits performed in this paper assume that the R-band template is adequately described by stretch. The effects of this on any results of this paper will be small, as the R-band template was only used for the two supernovae at $z \sim 0.18$. For one of these two supernovae, although the χ^2 for the lightcurve fit is poor, we have a very robust measurement of the peak R and I band magnitudes, and a robust stretch measurement (from the R-band lightcurve, which is a redshifted V-band lightcurve).

Add this, if it's true. Or modify it, if not, but keep the wording positive like this if possible.

Some of the high-redshift supernovae lack a supernova-free P99 host galaxy image. These supernovae were fit with an additional variable parameter: the zero-level of the I-band lightcurve.

Table 2: U, V, and R Lightcurve Templates Used

Day[a]	U flux[b]	V flux[b]	R flux[b]	Day[1]	U flux[b]	V flux[b]	R flux[b]
-19	6.712e-03	4.960e-03	5.779e-03	31	4.790e-02	2.627e-01	3.437e-01
-18	2.685e-02	1.984e-02	2.312e-02	32	4.524e-02	2.481e-01	3.238e-01
-17	6.041e-02	4.464e-02	5.201e-02	33	4.300e-02	2.345e-01	3.054e-01
-16	1.074e-01	7.935e-02	9.246e-02	34	4.112e-02	2.218e-01	2.887e-01
-15	1.678e-01	1.240e-01	1.445e-01	35	3.956e-02	2.099e-01	2.733e-01
-14	2.416e-01	1.785e-01	2.080e-01	36	3.827e-02	1.990e-01	2.592e-01
-13	3.289e-01	2.430e-01	2.832e-01	37	3.722e-02	1.891e-01	2.463e-01
-12	4.296e-01	3.174e-01	3.698e-01	38	3.636e-02	1.802e-01	2.345e-01
-11	5.437e-01	4.017e-01	4.681e-01	39	3.565e-02	1.721e-01	2.237e-01
-10	6.712e-01	4.960e-01	5.779e-01	40	3.506e-02	1.649e-01	2.137e-01
-9	7.486e-01	5.889e-01	6.500e-01	41	3.456e-02	1.583e-01	2.046e-01
-8	8.151e-01	6.726e-01	7.148e-01	42	3.410e-02	1.524e-01	1.962e-01
-7	8.711e-01	7.469e-01	7.725e-01	43	3.365e-02	1.471e-01	1.884e-01
-6	9.168e-01	8.115e-01	8.236e-01	44	3.318e-02	1.423e-01	1.813e-01
-5	9.524e-01	8.660e-01	8.681e-01	45	3.266e-02	1.378e-01	1.747e-01
-4	9.781e-01	9.103e-01	9.062e-01	46	3.205e-02	1.337e-01	1.687e-01
-3	9.940e-01	9.449e-01	9.382e-01	47	3.139e-02	1.299e-01	1.630e-01
-2	1.000e+00	9.706e-01	9.639e-01	48	3.072e-02	1.263e-01	1.578e-01
-1	9.960e-01	9.880e-01	9.834e-01	49	3.005e-02	1.229e-01	1.529e-01
0	9.817e-01	9.976e-01	9.957e-01	50	2.945e-02	1.195e-01	1.483e-01
1	9.569e-01	1.000e+00	1.000e+00	51	2.893e-02	1.161e-01	1.440e-01
2	9.213e-01	9.958e-01	9.952e-01	52	2.853e-02	1.128e-01	1.398e-01
3	8.742e-01	9.856e-01	9.803e-01	53	2.830e-02	1.096e-01	1.359e-01
4	8.172e-01	9.702e-01	9.545e-01	54	2.827e-02	1.064e-01	1.320e-01
5	7.575e-01	9.502e-01	9.196e-01	55	2.849e-02	1.033e-01	1.282e-01
6	6.974e-01	9.263e-01	8.778e-01	56	2.793e-02	1.003e-01	1.244e-01
7	6.375e-01	8.991e-01	8.313e-01	57	2.738e-02	9.743e-02	1.207e-01
8	5.783e-01	8.691e-01	7.821e-01	58	2.684e-02	9.467e-02	1.170e-01
9	5.205e-01	8.369e-01	7.324e-01	59	2.630e-02	9.207e-02	1.133e-01
10	4.646e-01	8.031e-01	6.842e-01	60	2.578e-02	8.964e-02	1.097e-01
11	4.113e-01	7.683e-01	6.396e-01	61	2.527e-02	8.741e-02	1.061e-01
12	3.610e-01	7.330e-01	6.007e-01	62	2.477e-02	8.538e-02	1.026e-01
13	3.145e-01	6.977e-01	5.691e-01	63	2.428e-02	8.359e-02	9.910e-02
14	2.725e-01	6.629e-01	5.444e-01	64	2.380e-02	8.207e-02	9.568e-02
15	2.356e-01	6.293e-01	5.254e-01	65	2.333e-02	8.083e-02	9.232e-02
16	2.044e-01	5.972e-01	5.113e-01	66	2.287e-02	7.927e-02	8.902e-02
17	1.783e-01	5.667e-01	5.011e-01	67	2.242e-02	7.774e-02	8.579e-02
18	1.567e-01	5.376e-01	4.938e-01	68	2.197e-02	7.624e-02	8.264e-02
19	1.388e-01	5.099e-01	4.887e-01	69	2.154e-02	7.476e-02	7.958e-02
20	1.239e-01	4.835e-01	4.848e-01	70	2.111e-02	7.332e-02	7.660e-02
21	1.115e-01	4.583e-01	4.814e-01	71	2.070e-02	7.191e-02	7.373e-02
22	1.008e-01	4.342e-01	4.776e-01	72	2.029e-02	7.052e-02	7.096e-02
23	9.144e-02	4.113e-01	4.725e-01	73	1.989e-02	6.916e-02	6.832e-02
24	8.314e-02	3.894e-01	4.653e-01	74	1.949e-02	6.782e-02	6.581e-02
25	7.583e-02	3.685e-01	4.552e-01	75	1.911e-02	6.651e-02	6.344e-02
26	6.941e-02	3.486e-01	4.414e-01	76	1.873e-02	6.523e-02	6.199e-02
27	6.380e-02	3.296e-01	4.247e-01	77	1.836e-02	6.397e-02	6.057e-02
28	5.891e-02	3.115e-01	4.058e-01	78	1.799e-02	6.274e-02	5.918e-02
29	5.467e-02	2.943e-01	3.855e-01	79	1.764e-02	6.153e-02	5.783e-02
30	5.102e-02	2.781e-01	3.645e-01	80	1.729e-02	6.034e-02	5.650e-02

a: Day is relative to the epoch of the maximum of the B-band lightcurve.
b: Relative fluxes.

I can't find 94G on any o fthe tables. Is it a typo, or is the mistake in the tables?

The supernovae treated in this manner include SN 1997J, SN 1997O, SN 1997Q, SN 1997R, SN 1997S, SN 1997K, and SN 1997am. Both R and I band zero offsets were allowed to vary for SN 1994G.

The late-time lightcurve behavior may bias the result of a lightcurve fit (Aldering, Knop, & Nugent 2000); it is therefore important that the low and high-redshift supernovae be treated in as consistent a manner as possible. Few or none of the high-redshift supernovae have high-precision measurements ∼40–50 days after maximum light, so as in Perlmutter *et al.* (1997) and P99 these late-time points were eliminated from the low-redshift lightcurve data before the template fit procedure. Additionally, to allow for systematic offset uncertainties on the host galaxy subtraction, an "error floor" of 0.007 times the maximum lightcurve flux was applied; any point with an uncertainty below the error floor had its uncertainty replaced by that value (Goldhaber *et al.* 2001).

The final results of the lightcurve fits, including the effect of color corrections and K-corrections, are listed in Table 3 for the 11 supernovae of this paper. Table 4 shows the results of new lightcurve fits for the 42 high-redshift supernovae of P99, and Table 5 shows the results of lightcurve fits for the low-redshift supernovae from H96 and R99. Appendix A tabulates all of the lightcurve data and shows plots of all of the lightcurves for the SNe in this paper.

2.3. Color- and K-Corrections

In order to combine data from different telescopes, icolor corrections were applied to remove the differences in the spectral responses of the filters relative to the Bessell system (Bessell 1990). For the ground-based telescopes, the filters are close enough to the standard Bessell filters that a single linear color term (measured at each observatory with standard stars) suffices to put the data onto the Bessell system, with most corrections being smaller than 0.01 magnitudes. The WFPC2 filters are different enough from the ground-based filters, however, that a linear term is not sufficient. Moreover, the differences between a SN Ia and standard star spectral energy distribution (SED) are significant. In this case, color corrections were calculated by integrating template SN Ia spectra (described below).

In order to perform lightcurve template fitting, a cross-filter K-correction (Kim, Goobar, & Perlmutter 1996) must be applied to transform the data in the observed filter into a rest-frame magnitude in the filter used for the lightcurve template. The color correction to the nearest standard Bessell filter followed by a K-correction to a rest-frame filter is equivalent to a direct K-correction from the observed filter to the standard rest-frame filter. In practice, we perform the two steps separately so that all photometry may be combined to provide a lightcurve effectively observed through a standard (e.g.) R-band filter, which may then be K-corrected and fit with a single series of K-corrections.

Color and K-corrections were performed following the procedure of Nugent, Kim, & Perlmutter (2002). In order to perform these corrections, a template SN Ia spectrum for each epoch of the lightcurve, as described in that paper, is necessary. The spectral template used in this present paper began with the template of that paper. To it was applied a smooth multiplicative function at each day such ~~to ensure~~ that integration of the spectrum through the standard filters would produce the proper intrinsic colors for a Type Ia supernova (including a mild dependence of those intrinsic colors on stretch).

Is this necessary at all if we later use *measured* color to re-tilt spectra? If not, this will confuse the reader.

The proper intrinsic colors for the supernova spectral template were determined in the $BVRI$ spectral range by smooth fits to the low-redshift supernova data of H96 and R99. For each color (B-V, V-R, and R-I), every data point from those papers was K-corrected and corrected for Galactic extinction. These data were plotted together, and then a smooth curve was fit to the plot of color versus date relative to maximum. This curve is given by two parameters, each of which was a function of time, and is described by a spline under tension: an "intercept" $b(t)$ and a "slope" $m(t)$. At any given date the intrinsic color is

$$color(t') = b(t') + m(t') \times 1/s \qquad (2)$$

where $t' = t/(s(1+z))$, z is the redshift of the supernova, and s is the timescale stretch of the supernova from a simultaneous fit to the B and V lightcurves (matching the procedure used for most of the high redshift supernovae). As the goal was to determine intrinsic colors without making any assumptions about reddening, no host-galaxy extinction

Table 3: Supernova Lightcurve Fits: HST Supernovae from this paper

from

SN	z	$m_X{}^a$	$m_B{}^b$	Stretch	R-I^c	$E(B$-$V)$ Gal.^{d}	$E(B$-$V)^e_{\rm host}$	Excluded Subsets^f
1997ek	0.863	23.39	24.58 ± 0.03	1.052 ± 0.002	0.831 ± 0.066	0.042	0.125 ± 0.096	
1997eq	0.538	22.65	23.23 ± 0.03	0.987 ± 0.031	0.151 ± 0.034	0.044	0.036 ± 0.038	
1997ez	0.778	23.27	24.39 ± 0.04	1.056 ± 0.038	0.696 ± 0.061	0.026	0.088 ± 0.089	
1998as	0.355	22.20	22.71 ± 0.03	0.942 ± 0.020	0.166 ± 0.032	0.037	0.082 ± 0.035	
1998aw	0.440	22.64	23.29 ± 0.02	1.025 ± 0.021	0.286 ± 0.028	0.026	0.227 ± 0.030	2,3
1998ax	0.497	22.59	23.20 ± 0.05	1.100 ± 0.034	0.123 ± 0.049	0.035	0.003 ± 0.053	
1998ay	0.638	23.28	23.91 ± 0.08	1.054 ± 0.047	0.250 ± 0.072	0.035	0.100 ± 0.091	
1998ba	0.430	22.34	22.94 ± 0.05	0.921 ± 0.023	0.057 ± 0.042	0.024	0.023 ± 0.045	
1998be	0.644	23.31	23.89 ± 0.04	0.761 ± 0.033	0.406 ± 0.056	0.029	0.073 ± 0.072	
1998bi	0.740	22.95	24.00 ± 0.03	0.951 ± 0.035	0.526 ± 0.045	0.026	0.002 ± 0.063	
2000fr	0.543	22.52	23.14 ± 0.03	1.076 ± 0.013	0.104 ± 0.032	0.030	0.079 ± 0.036	

a: Magnitude in the observed filter at the peak of the rest-frame B-band lightcurve. X=R for $z < 0.7$, X=I for $z > 0.7$.
b: This value has been K-corrected and corrected for Galactic $E(B$-$V)$ extinction.
c: This is the observed R-I color at the epoch of the rest-frame B-band lightcurve peak.
d: Schlegel, Finkbeiner, & Davis (1998)
e: Measurement uncertainty only; no intrinsic color dispersion included.
f: The indicated supernovae were excluded from Subset 1 (full primary subset), Subset 2 (low-extinction primary subset), and/or Subset 3(low-extinction, strict SN Ia subset); see § 2.4.

Say how big this error bar is quantitatively

corrections were applied to the literature data at this stage of the analysis. Instead, host-galaxy extinction was handled by fitting the blue side ridge-line of the supernova color curves, so as to extract the unreddened intrinsic color. This ridge-line fit was performed by adding an asymmetric intrinsic error bar (twice as long to the red than to the blue), and by omitting supernovae from the fit which were systematically reddened relative to the median value.

Some of our data extends into the U-band range of the spectrum. This is obvious for supernovae at $z > 0.7$ where a U-band template is fit to the R-band data. However, even for supernovae at $z \gtrsim 0.55$, the de-redshifted R-band filter begins to overlap the U-band range of the rest-frame spectrum. Thus, it is also important to know the intrinsic U-B color so as to generate a proper spectral template. We used data from the literature in Table 6. Here, there is an insufficient number of supernova lightcurves to reasonably use the sort of ridge-line analysis used above to eliminate the effects of host-galaxy extinction in determining the intrinsic $BVRI$ colors. Instead, for U-B, we perform extinction corrections using the $E(B$-$V)$ values from Phillips *et al.* (1999). Based on Table 6, we adopt a U-B color of 0.4 at the epoch of rest-B maximum. Although any intrinsic uncertainty in B-V should be included in the assumed intrinsic dispersion of extinction-corrected peak magnitudes (see § 2.5), it is likely that there is a greater intrinsic dispersion in U-B. The effect on extinction-corrected magnitudes will be further increased by the greater effect of dust extinction on the bluer U-band light. The scatter of our extinction-corrected magnitudes about the best fit cosmology suggests an intrinsic uncertainty in U-B of 0.04 magnitudes. This is also consistent with the U-B data of Jha (2003) over the range of timescale stretch of our $z > 0.6$ SNe Ia, after two extreme color outliers are removed. There is no evidence of such extreme color objects in our dataset. Note that this intrinsic color dispersion is in addition to the intrinsic magnitude dispersion assumed after extinction correction.

Given a template spectrum with the proper intrinsic colors for each day relative to the date of B maximum, it must be further modified for each supernova to account for dust extinction in the supernova host galaxy, and extinction of the redshifted spectrum due to Galactic dust. Reddening effects from dust were calculated given the $E(B$-$V)$ parameter (measured from the lightcurve fits for the host galaxy, and given by Schlegel, Finkbeiner, & Davis (1998) for the Galaxy) and the extinction law of O'Donnell (1994).

Re-word this sentence. Confusing.

For each supernova, this finally modified spectral template was integrated through the Bessell and WFPC2 filter transmission functions to provide color and K-corrections. The exact spectral template needed for a given data point on a given

This value is also consistant with the data shown in Jha (2003) for supernovae with timescale stretch of s ~ 1, although the data is not determinative (see Section 5.4 for the effect of systematic error in this value).

Reminder of a check that should be done (probably while the paper is being refereed): Now that we know what fits we are using and we have this table, we need to see how much mag and stretch have changed since P99. If there are a few bad changes (aside from the SNe that we are now throwing out of the fits -- and probably removing from this table, with just a footnote telling why they are gone) then we should probably add a sentence or two to the paper when it comes back from the referee explaining what happened.

Table 4: Supernova Lightcurve Fits: New Fits to Perlmutter (1999) SNe

from

SN	z	m_X[a]	m_B[b]	Stretch	R-I[c]	$E(B$-$V)$ Gal.[d]	$E(B$-$V)^e_{\rm host}$	Excluded Subsets[f]
1992bi	0.458	22.13	22.81 ± 0.09	0.860 ± 0.451	—	0.010	—	1–3
1994F	0.354	22.06	22.55 ± 0.14	0.690 ± 0.142	—	0.036	—	1–3
1994H	0.374	21.31	21.84 ± 0.03	0.876 ± 0.033	—	0.031	—	1–3
1994al	0.420	22.37	22.68 ± 0.05	1.035 ± 0.147	—	0.136	—	1–3
1994am	0.372	21.81	22.33 ± 0.04	0.886 ± 0.002	—	0.031	—	1–3
1994an	0.378	22.13	22.57 ± 0.07	1.017 ± 0.119	—	0.066	—	1–3
1995aq	0.453	22.61	23.25 ± 0.07	0.870 ± 0.100	0.029 ± 0.132	0.022	0.079 ± 0.139	1–3
1995ar	0.465	22.80	23.49 ± 0.08	0.915 ± 0.111	0.509 ± 0.233	0.022	0.433 ± 0.255	
1995as	0.498	23.03	23.68 ± 0.07	1.038 ± 0.091	0.153 ± 0.205	0.021	0.033 ± 0.222	3
1995at	0.655	22.62	23.25 ± 0.03	1.050 ± 0.064	0.350 ± 0.109	0.019	0.003 ± 0.139	1–3
1995aw	0.400	21.79	22.28 ± 0.03	1.186 ± 0.037	0.116 ± 0.103	0.040	0.159 ± 0.108	
1995ax	0.615	22.54	23.21 ± 0.06	1.129 ± 0.071	0.120 ± 0.211	0.033	0.200 ± 0.259	
1995ay	0.480	22.64	23.05 ± 0.04	0.881 ± 0.066	0.206 ± 0.164	0.114	0.021 ± 0.177	
1995az	0.450	22.46	22.66 ± 0.07	0.973 ± 0.066	0.085 ± 0.138	0.181	0.118 ± 0.148	
1995ba	0.388	22.08	22.65 ± 0.05	0.970 ± 0.046	0.013 ± 0.106	0.018	0.040 ± 0.112	
1996cf	0.570	22.70	23.30 ± 0.03	1.000 ± 0.050	0.152 ± 0.093	0.040	0.078 ± 0.109	3
1996cg	0.490	22.46	23.09 ± 0.03	1.013 ± 0.041	0.299 ± 0.101	0.035	0.186 ± 0.110	3
1996ci	0.495	22.19	22.82 ± 0.02	0.966 ± 0.045	0.081 ± 0.071	0.028	0.054 ± 0.076	
1996ck	0.656	23.09	23.76 ± 0.05	0.888 ± 0.077	0.189 ± 0.262	0.032	0.227 ± 0.333	
1996cl	0.828	23.37	24.52 ± 0.16	0.963 ± 0.234	0.550 ± 0.188	0.035	0.362 ± 0.265	
1996cm	0.450	22.67	23.26 ± 0.07	0.899 ± 0.065	0.212 ± 0.180	0.049	0.103 ± 0.193	3
1996cn	0.430	22.58	23.25 ± 0.03	0.892 ± 0.064	0.375 ± 0.091	0.025	0.313 ± 0.100	2,3
1997F	0.580	22.91	23.49 ± 0.06	1.050 ± 0.068	0.249 ± 0.205	0.040	0.023 ± 0.244	
1997G	0.763	23.48	24.41 ± 0.40	0.825 ± 0.096	0.094 ± 0.447	0.043	0.708 ± 0.600	
1997H	0.526	22.69	23.25 ± 0.03	0.887 ± 0.050	0.295 ± 0.181	0.051	0.125 ± 0.203	
1997I	0.172	20.18	20.41 ± 0.01	0.965 ± 0.009	0.072 ± 0.047	0.051	0.086 ± 0.066	
1997J	0.619	23.21	23.84 ± 0.06	1.038 ± 0.124	0.167 ± 0.342	0.039	0.160 ± 0.423	
1997K	0.592	23.78	24.42 ± 0.12	1.083 ± 0.159	0.280 ± 0.356	0.020	0.053 ± 0.429	1–3
1997L	0.550	22.90	23.52 ± 0.05	0.938 ± 0.058	—	0.025	—	1–3
1997N	0.180	20.40	20.49 ± 0.02	1.070 ± 0.016	0.090 ± 0.096	0.031	0.089 ± 0.130	
1997O	0.374	23.00	23.53 ± 0.07	1.045 ± 0.069	0.085 ± 0.157	0.029	0.036 ± 0.169	1–3
1997P	0.472	22.53	23.15 ± 0.04	0.890 ± 0.039	0.054 ± 0.218	0.033	0.074 ± 0.231	
1997Q	0.430	22.01	22.61 ± 0.02	0.935 ± 0.024	0.068 ± 0.145	0.030	0.014 ± 0.154	
1997R	0.657	23.28	23.88 ± 0.05	0.980 ± 0.065	0.354 ± 0.182	0.030	0.013 ± 0.233	
1997S	0.612	23.03	23.89 ± 0.05	1.189 ± 0.073	0.424 ± 0.411	0.033	0.851 ± 0.495	
1997ac	0.320	21.43	21.89 ± 0.02	1.057 ± 0.020	0.059 ± 0.066	0.027	0.003 ± 0.073	
1997af	0.579	22.92	23.59 ± 0.08	0.856 ± 0.052	0.007 ± 0.238	0.028	0.268 ± 0.281	
1997ai	0.450	22.27	22.86 ± 0.07	0.926 ± 0.116	0.136 ± 0.138	0.045	0.029 ± 0.147	
1997aj	0.581	22.58	23.24 ± 0.11	0.956 ± 0.055	0.013 ± 0.173	0.033	0.260 ± 0.205	
1997am	0.416	22.02	22.58 ± 0.07	1.030 ± 0.060	0.046 ± 0.114	0.036	0.016 ± 0.121	
1997ap	0.830	23.18	24.36 ± 0.08	1.003 ± 0.066	0.920 ± 0.087	0.026	0.178 ± 0.131	
199fG	0.425	21.64	22.30 ± 0.16	0.924 ± 0.186	0.071 ± 0.163	0.008	0.008 ± 0.173	

a: X=R for $z < 0.7$, X=I for $z > 0.7$

b: As in Table 3

c: As in Table 3

d: Schlegel, Finkbeiner, & Davis (1998)

e: As in Table 3

f: The indicated supernovae were excluded from Subset 1 (full primary subset), Subset 2 (low-extinction primary subset), and/or Subset 3(low-extinction, strict SN Ia subset); see § 2.4.

Table 5: Supernova Lightcurve Fits: Low-z SNe from Hamuy (1996) and Riess (1999) from

SN[a]	z	m_B[b]	Stretch	B-V[c]	$E(B$-$V)$ Gal.[d]	$E(B$-$V)^e_{\rm host}$	Excluded Subsets[f]
1990O	0.030	16.14 ± 0.03	1.113 ± 0.027	0.038 ± 0.027	0.098	0.023 ± 0.028	
1990af	0.050	17.76 ± 0.01	0.752 ± 0.010	0.073 ± 0.011	0.035	0.002 ± 0.012	
1992P	0.026	16.04 ± 0.02	1.071 ± 0.027	0.049 ± 0.019	0.020	0.028 ± 0.019	
1992ae	0.075	18.39 ± 0.03	0.968 ± 0.026	0.075 ± 0.027	0.036	0.031 ± 0.030	
1992ag	0.026	16.23 ± 0.02	1.061 ± 0.016	0.215 ± 0.021	0.097	0.163 ± 0.021	2,3
1992al	0.014	14.47 ± 0.01	0.960 ± 0.011	0.055 ± 0.013	0.034	0.045 ± 0.013	
1992aq	0.101	19.28 ± 0.05	0.895 ± 0.030	0.094 ± 0.031	0.012	0.071 ± 0.036	
1992bc	0.020	15.09 ± 0.01	1.056 ± 0.006	0.092 ± 0.009	0.022	0.067 ± 0.009	
1992bg	0.036	16.61 ± 0.04	1.013 ± 0.015	0.121 ± 0.026	0.181	0.040 ± 0.027	
1992bh	0.045	17.59 ± 0.02	1.029 ± 0.016	0.098 ± 0.018	0.022	0.083 ± 0.019	
1992bl	0.043	17.30 ± 0.03	0.820 ± 0.013	0.005 ± 0.023	0.012	0.024 ± 0.024	
1992bo	0.018	15.77 ± 0.01	0.758 ± 0.007	0.052 ± 0.012	0.027	0.036 ± 0.012	
1992bp	0.079	18.27 ± 0.01	0.911 ± 0.015	0.067 ± 0.015	0.068	0.089 ± 0.017	
1992br	0.088	19.33 ± 0.08	0.704 ± 0.024	0.158 ± 0.050	0.027	0.011 ± 0.056	1–3
1992bs	0.063	18.18 ± 0.04	1.050 ± 0.015	0.016 ± 0.021	0.013	0.070 ± 0.023	
1993B	0.071	18.35 ± 0.04	1.037 ± 0.019	0.163 ± 0.027	0.080	0.039 ± 0.029	
1993O	0.052	17.63 ± 0.01	0.930 ± 0.009	0.036 ± 0.012	0.053	0.036 ± 0.013	
1993ag	0.050	17.80 ± 0.02	0.949 ± 0.016	0.208 ± 0.020	0.111	0.092 ± 0.021	
1994M	0.024	16.23 ± 0.03	0.887 ± 0.015	0.037 ± 0.022	0.023	0.041 ± 0.022	
1994S	0.016	14.77 ± 0.02	1.035 ± 0.026	0.064 ± 0.019	0.018	0.030 ± 0.019	
1995ac	0.049	17.03 ± 0.01	1.090 ± 0.013	0.014 ± 0.011	0.042	0.032 ± 0.012	
1995bd	0.016	15.18 ± 0.01	1.040 ± 0.008	0.734 ± 0.008	0.490	0.299 ± 0.008	1–3
1996C	0.030	16.54 ± 0.04	1.125 ± 0.019	0.002 ± 0.026	0.014	0.024 ± 0.027	
1996ab	0.125	19.52 ± 0.04	0.961 ± 0.036	0.111 ± 0.032	0.032	0.153 ± 0.038	
1996bl	0.035	16.64 ± 0.01	1.033 ± 0.015	0.086 ± 0.012	0.099	0.009 ± 0.012	
1996bo	0.016	15.83 ± 0.01	0.862 ± 0.006	0.404 ± 0.008	0.077	0.360 ± 0.008	1–3

a: Supernovae through 1993ag are from H96, later ones from R99.

b: Measurement uncertainties as for note 2 in Table 3.

c: This is the measured B-V color at the epoch of rest-frame B-band lightcurve maximum. d: Schlegel, Finkbeiner, & Davis (1998)

e: Measurement error only; no intrinsic color dispersion included.

f: The indicated supernovae were excluded from Subset 1 (full primary subset), Subset 2 (low-extinction primary subset), and/or Subset 3(low-extinction, strict SN Ia subset); see § 2.4.

Table 6: U-B SN Ia Colors at Epoch of B-band Maximum

SN	Raw U-B^1	Corrected U-B^2	Reference
1980N	0.21	0.29	Hamuy *et al.* (1991)
1989B	0.08	0.33	Wells *et al.* (1994)
1990N	0.35	0.45	Lira *et al.* (1998)
1994D	0.50	0.52	Wu *et al.* (1995)
1998bu	0.23	0.51	Suntzeff *et al.* (1999)

1: This is the measured U-B value from the paper

2: This is U-B K-corrected, and corrected for host galaxy and Galactic extinction

supernova is dependent on parameters of the fit: the stretch, the time of each point relative to the epoch of rest-B maximum, and the host-galaxy $E(B$-$V)$ (measured from the peak color of the lightcurve). Thus, color and K-corrections were performed iteratively with lightcurve fitting in order to generate the final corrections used in the fits described in § 2.2. An initial date of maximum, stretch, and host-galaxy extinction was assumed to generate K-corrections for the first iteration of the fit. The parameters resulting from that fit were used to generate new color and K-corrections, and the whole procedure was repeated until the results of the fit converged. Generally, the fit converged within 2–3 iterations, although occasionally a few more iterations were necessary.

The $E(B$-$V)$ values quoted in Tables 3, 4, and 5 are the parameters for the extinction law of O'Donnell (1994) necessary to reproduce the observed R-I color at the epoch of the maximum of the rest-frame B lightcurve. This ~~reproduction~~ fit to observed R-I was performed by modifying the spectral template exactly as described above, given the intrinsic color of the supernova of the fit stretch, the Galactic extinction, and the host-galaxy $E(B$-$V)$ parameter. The modified spectrum was integrated through the Bessell R and I band filters, and $E(B$-$V)$ was varied until the R-I value produced matched the result from the lightcurve fit. (These $E(B$-$V)$ values where then used to generate the proper color and K-corrections for the next iteration of each lightcurve fit.)

2.4. Supernova Subsets

In P99, separate analyses were perfomed and compared for the supernova sample before and after removing supernovae with less secure identification as Type Ia. The results were shown to be consistent, providing a cross-check of the cosmological conslusions. For this current paper's analysis, adding and comparing eleven very-well-measured SNe Ia, we take the more securely identified SNe Ia as our primary sample. This excludes six supernoave from P99 (SNe 1992bi, 1994G, 1994al, 1995a1995aq, 1995at, and 1997K) that are very likely to be SNe Ia, but without good spectra confirmation, and one supernova (SN 1994H) that is considered a likely Type II supernova (Nugent, Kim, & Perlmutter 2002), and was removed from the primary P99 fits. Following P99, we omit two supernovae that are outliers in the stretch distribution, with $s < 0.75$ (SN 1992br and SN 1994F), and three supernova which are $> 4\,\sigma$ outliers from the best-fit flat-universe cosmology (SN 1996bo, SN 1995bd, and SN 1997O). Finally, we omit any supernovae ~~not yet omitted~~ which do not have a color measurement (SN 1994an, SN 1994am, and SN 1997L). The resulting "full primary subset" of SNe Ia, "Subset 1", is further culled to remove likely reddened supernovae, producing a "low-extinction primary subset," Subset 2. This subset omits three supernovae with host galaxy $E(B$-$V)> 0.1$ and $> 3\quad\sigma$ above zero (SN 1992ag, SN 1996cn, and SN 1998aw).

[Fix typo]

Subset 3, the "low-extinction strict Ia subset," makes an even more stringent cut on spectral confirmation, including only those supernovae whose confirmations as Type Ia SNe are unquestionable ~~(which includes all supernovae from this paper).~~ The additional supernovae omitted from Subset 3 beyond those omitted from Subset 2 are SN 1995as, SN 1996cf, SN 1996cg, and SN 1996cm. [...and SNe from this paper that we might now want to exclude from subset 3]

2.5. Cosmological Fit Methodology

Cosmological fits to the luminosity distance modulus equation from the Friedmann-Robertson-Walker metric followed the procedure of P99. The set of supernova redshifts (z) and K-corrected peak B-magnitudes (m_B) were fit to the equation

$$m_B = \mathcal{M} + 5\log \mathcal{D_L}(z; \Omega_\mathrm{M}, \Omega_\Lambda) \quad \alpha(s \quad 1) \quad (3)$$

where s is the stretch value for the supernova, $\mathcal{D_L} \equiv H_0 d_L$ is the "Hubble-constant-free" luminosity distance (Perlmutter *et al.* 1997), and $\mathcal{M} \equiv M_B \quad 5logH_0 + 25$ is the "Hubble-constant-free" B-band peak absolute magnitude of a $s = 1$ SN Ia. The peak magnitude of a SN Ia is mildly dependent on the lightcurve decay time scale, such that SNe with a slower decay (higher stretch) tend to be over-luminous, while SNe with a faster decay (lower stretch) tend to be under-luminous [Insert semi-colon] (Phillips *et al.* 1993); α is a slope that parameterizes this relationship.

There are four parameters in the fit: the mass density Ω_M and cosmological constant Ω_Λ, as well as the two nuisance parameters $\mathcal{M}$ and α. The four-dimensional (Ω_M, Ω_Λ, $\mathcal{M}$, α) space was divided into a grid, and at each grid point a χ^2 value was calculated by fitting the luminosity distance equation to the peak B-band magnitudes and redshifts of the supernovae. The range of parameter space explored included $\Omega_\mathrm{M} = [0, 3)$, $\Omega_\Lambda = [\quad 1, 3)$ (for fits where host-galaxy extinction corrections are not directly applied) or $\Omega_\mathrm{M} = [0, 4]$, $\Omega_\Lambda = [\quad 1, 4)$ (for fits with host-galaxy extinction corrections). No further constraints were placed on the parameters. An additional two dimensions on the grid included the relevant range for $\mathcal{M}$ and α. The probability of the whole 4-dimensional grid is normalized, and then integrated over the two dimensions corresponding to the "nuisance" parameters.

Fits were performed to the supernovae subsets described in § 2.4. These subset fits were also performed separately for the eleven high-redshift supernovae from this paper and for the 42 high-redshift supernovae from P99. Table 8 presents a summary of the results from these fits.

For each fit, all peak m_B values were corrected for Galactic extinction using $E(B\text{-}V)$ values from Schlegel, Finkbeiner, & Davis (1998), using the extinction law of O'Donnell (1994) integrated through the *observed* filter.[25] For fits of the low-extinction subsets (Subsets 2 and 3), the total effective statistical uncertainty on each value of m_B included the following contributions:

- the uncertainty on m_B from the lightcurve fits;
- the uncertainty on s, multiplied by α
- the covariance between m_B and s;
- a contribution from the uncertainty in the redshift due to peculiar velocity (assumed to have a dispersion of 300 km s $^{\ 1}$);
- 10% of the Galactic extinction correction; and
- 0.17 magnitudes of intrinsic dispersion (H96).

Fits to the full primary subset (Subset 1), which explicitly performed host-galaxy extinction corrections, used the first five items above plus:

- the uncertainty on $E(B\text{-}V)$ multiplied by R_B;
- the covariance between $E(B\text{-}V)$ and m_B;
- 0.11 magnitudes of intrinsic dispersion (Phillips *et al.* 1999); and
- 0.04 magnitudes of intrinsic U-B dispersion (see below).

Host-galaxy extinction corrections used a value $R_B \equiv A_B/E(B\text{-}V) = 4.34$, which results from applying the extinction law of O'Donnell (1994) to a SN Ia spectrum and integrating the results through standard B and V filters. Although there is almost certainly some intrinsic dispersion either in the proper value of R_B to use, or in the true B-V color of a SN Ia (Nobili *et al.* 2003), we do not explicitly include such a term. The effects of such a dispersion should be included in the 0.11 magnitudes of intrinsic magnitude dispersion which Phillips *et al.* (1999) see after applying extinction corrections. As discussed in § 2.3, the intrinsic U-B dispersion is likely to be greater than the intrinsic B-V dispersion. For those supernovae most affected by this (i.e. those at $z > 0.7$), we included an additional uncertainty in magnitude corresponding to 0.04 magnitudes of intrinsic U-B

[25] This supersedes P99, where an incorrect dependence of the effective on R_R for Galactic extinction was applied. The corrected procedure decreases the flat-universe value of Ω_M by 0.03.

dispersion, converted into a magnitude error using the O'Donnell extinction law. This set of statistical uncertainties is slightly different from those used in P99. For these fits, at each test value of α we propagated the stretch errors into the corrected B-band magnitude errors; in contrast, P99 used a single value of $\alpha = 1.74$ for purposes of error propagation.

3. Colors and Extinction

For the primary fit of our P99 analysis,

One notable difference between the data on the 11 WFPC2-observed supernovae in this paper and previous high-redshift supernova data is that the R-I colors have been measured to much higher precision. ~~In the work of the SCP (P99),~~ extinction was estimated by comparing the mean host-galaxy $E(B\text{-}V)$ values from the low and high redshift samples. Although the uncertainties on individual $E(B\text{-}V)$ values for high-redshift supernovae were relatively large, the uncertainty on the mean of the distribution was only 0.01 magnitudes. P99 showed that there was no significant difference in the mean host-galaxy reddening between the low and high redshift sets of supernovae of the primary analysis (Fit C). This tightly constrained the systematic uncertainty on the cosmological results due to differences in extinction. Fit E of P99 and Riess (1998) did apply host-galaxy extinction corrections to each individual supernova. However, these analyses used a Bayesian prior on the color-excess distribution to modify the extinction correction. This prior was one sided, with zero probability for $E(B\text{-}V) < 0$, and a probability which sharply falls for positive values of $E(B\text{-}V) > 0.02$ magnitudes (Hatano, Branch, & Deaton 1998). Even if all $E(B\text{-}V)$ values are intrinsically close to zero, measurements will scatter to both sides of zero by an amount given by the measurement uncertainty; consequently, applying this asymmetric prior biases the measured $E(B\text{-}V)$ distribution to the red. As discussed in P99, when the uncertainties on the high and low redshift supernova $E(B\text{-}V)$ values differ, this prior ~~can~~ introduces a bias into the cosmological results; P99 therefore cautioned against this approach. ~~(The validity of a prior with such small dispersion is further called into question by the observation that a number of the low-redshift supernovae in R99 were found with moderate amounts of host-galaxy extinction.)~~

[[Greg thinks the Hatano prior is consistent with the R99 reddened SNe, so delete this parenthesis.]]

The small dispersion of the prior makes the cosmological fits appear much better constrained by reducing the propagated $E(B\text{-}V)$ measurement uncertainties, especially for SNe with $E(B\text{-}V) < 0$ (as was the case for more than half of the SNe in Riess (1998)).

Table 7: Mean $E(B\text{-}V)$ Values

Low-Extinction Primary Subset (Subset 2) SNe

Set	All SNe	~~Subset 2~~ SNe[1]
Low z:		
H96	0.015 ± 0.004	0.021 ± 0.004
R99	$+0.193 \pm 0.004$	0.011 ± 0.007
High z:		
P99	$+0.009 \pm 0.024$	0.008 ± 0.026
This Paper	$+0.044 \pm 0.014$	0.008 ± 0.016

1: SNe omitted from Fits 1–3 (§ 4.1, Table 8) have been omitted from these means. This excludes outliers, as well as supernovae with $E(B\text{-}V) > 3\sigma$ above zero.

The high precision measurements of the R-I color afforded by the WFPC2 lightcurves for the supernovae in this work allow a direct estimation of the host-galaxy $E(B\text{-}V)$ color excess without any need to resort to a prior assumption in the intrinsic color-excess distribution.

Figure 1 shows histograms of the host-galaxy $E(B\text{-}V)$ values from different subsets of supernovae. For the bottom two panels, ~~over-plotted is a line~~ a line is over-plotted that treats the H96 SNe $E(B\text{-}V)$ values as a parent distribution, and shows the expected distribution for the other sets given their measurement uncertainties. Each set's distribution is consistent with the $E(B\text{-}V)$ distribution from H96, except for R99 which shows several significantly reddened supernovae. ~~This effect arises because~~ The R99 SNe are not from a flux-limited sample, ~~as are the~~ and therefore are more likely to include extincted supernovae that would be selected against in flux limited samples such as H96 and all high redshift SNe. Flux-limited surveys select against extincted SNe. For the 11 HST SNe in this paper, one is significantly reddened (with $E(B\text{-}V) > 3\sigma$ above zero). [Start new paragraph here]] Table 7 lists the variance-weighted mean $E(B\text{-}V)$ values for each set. For the low-extinction Subset 1 the four sets are not significantly different. That the low-redshift supernovae are too blue indicate that the assumed B-V color at epoch of B maximum (determined from all of the low-redshift SNe from H96 and P99 following the procedure of § 2.3) may

Subset 2, [not 1]

Re-word!

Explain that this means not significantly enough to affect Omega_m and Omega_lambda by more than XXX (0.05??)

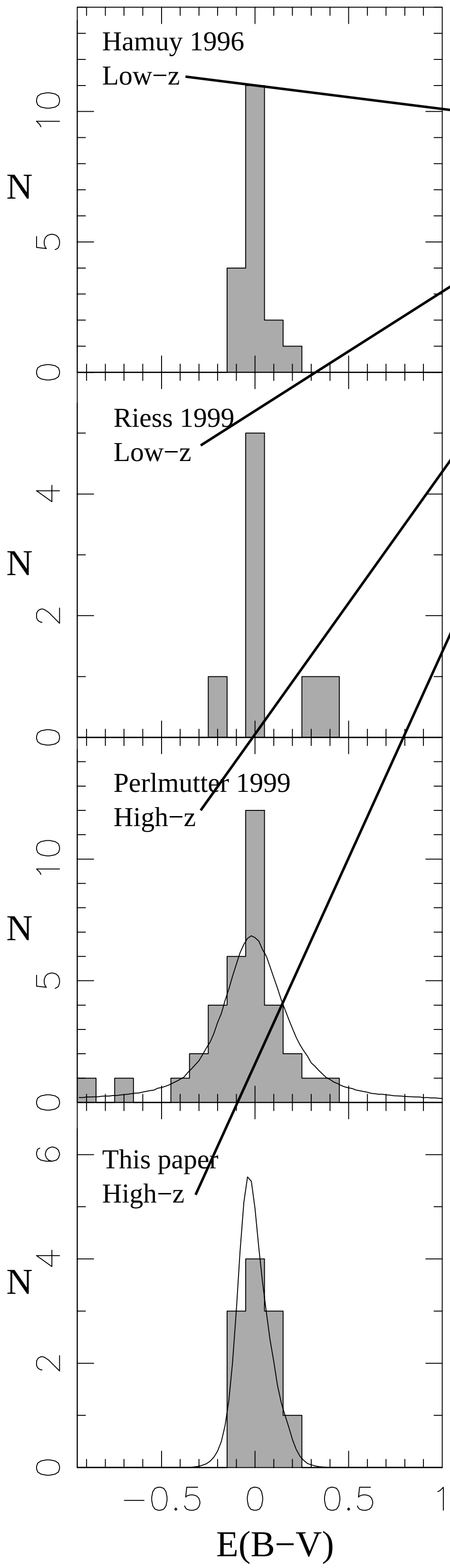

spell out "z" as "redshift" (so that readers don't think we mean "High-Z Team")

Fig. 1.— Histograms of $E(B\text{-}V)$ for the four sets of supernovae used in this paper. All supernovae with measured colors ~~(i.e. excluding seven from P99)~~ are plotted. The solid lines drawn over the bottom two panels is a simulation of the distribution expected if the H96 set represented the true distribution of SN colors, given the error bars of each set.

[[The Liebundgut paper (and Falco?) were not using z ~ 0.7 SNe, were they? The assumed B-V would have had to be too red, but you just said that this doesn't matter, since we take the difference between low and high-redshift SN samples for this restframe color. We elsewhere say that it might be the K-correction error due to U-B choice that caused the Liebundgut "too blue" problem, but then we show a graph of the effect of U-B on K-correction in Fig 8(c) that looks like it barely has any effect. We probably need to think through what our consistent interpretation is of all these questions.
Also we need to explain why an incorrect U-B color assumption would not cancel out as it does for B-V, since the low-redshift SN sets we use (H96,R99) do not have U-B measurements that could provide the cancelation.]]

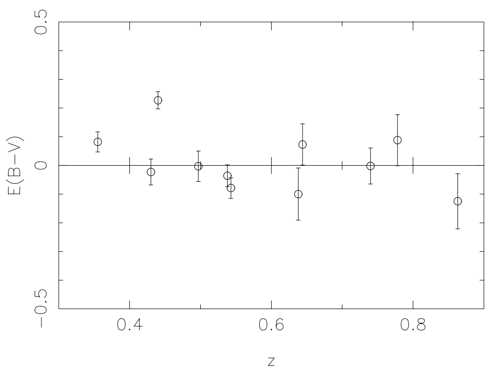

Fig. 2.— A plot of $E(B\text{-}V)$ as a function of redshift for the 11 HST-observed SNe of this paper shows that there is no trend of host-galaxy extinction with redshift. The only supernova with a significant color excess is SN 1998aw at $z = 0.44$.

Re-word this sentence, to make easier to understand

be mildly too red by ~ 0.02 magnitudes; we consider the effect that this might have on which supernovae are rejected for being reddened in § 5.3. [move up] Because it is a *difference* between the reddening of the low high and redshift supernovae that would systematically affect $\Omega_{\rm M}$ and Ω_Λ, any such small offset in assumed intrinsic color will ~~should~~ not affect those measurements.

[[Move this up above to just before the discussion in the previous paragraph of the "too blue" low -z SNe.]]

For the 11 HST supernovae in this paper, if SN 1998aw is omitted, then the mean $E(B\text{-}V)$ of the set is consistent as in Subset 2 with the mean $E(B\text{-}V)$ of the Subset 2 supernovae from both low-redshift sets. Note that this conclusion is not circular; individual $E(B\text{-}V)$ error bars for the HST supernovae are typically 0.04–0.1, and hence only grossly reddened supernovae have been omitted from Subset 2. A residual difference on the mean $E(B\text{-}V)$ value is still possible, but is not detected at the 0.015 mag level [??].

The mean host-galaxy color excess calculated for the highest redshift supernovae is critically dependent on the assumed intrinsic $U\text{-}B$ color. This is obvious for supernovae at $z > 0.7$, where the $E(B\text{-}V)$ value is estimated directly from measurements of the $U\text{-}B$ rest-frame color. Even for supernovae at $z \gtrsim 0.55$, the de-redshifted R filter overlaps part of the U band region of the rest-frame spectrum, and ~~as such~~ thus the assumed $U\text{-}B$ color will affect the cross-filter K-correction between observed R and rest-frame B.

Figure 2 shows $E(B\text{-}V)$ vs. z for the 11 supernovae of this paper. This figure graphically shows both that except for SN 1998aw at $z = 0.44$ (and to a lesser degree, SN 1998as at $z = 0.36$), the supernovae do not suffer from significant host-galaxy extinction. Those two supernovae which are reddened are at the low end of the redshift scale, which is as would be expected for a flux-limited survey. Several authors (including Leibundgut (2001) and Falco *et al.* (1999)) have suggested that there is evidence that high-redshift supernovae are bluer statistically than the low-redshift counterparts they are compared with. These data show no such effect. $\boxed{\text{It is possible that the problem was caused by an assumed intrinsic } U\text{-}B \text{ that was too red.}}$

In should be noted that K-corrected magnitudes are dependent on the assumed supernova colors that went into deriving the K-corrections. If the assumed $U\text{-}B$ color is too red, that will affect the cross-filter K-correction applied to R band data at $z \gtrsim 0.5$, thereby changing derived rest frame colors. In § 5, we consider the effect of changing the $U\text{-}B$ color assumed.

4. Cosmological Results

4.1. $\Omega_{\rm M}$ and Ω_Λ

Figure 3 shows Hubble Diagrams which plot K-corrected rest-frame B-band peak magnitudes and redshifts for the new supernovae of this paper. For most supernovae, the rest-frame peak B-band magnitude was calculated from the observed and K-corrected R-band lightcurve. For supernovae at $z > 0.7$, the peak rest-frame B magnitude was calculated from the peak of the I-band lightcurve. In the upper panel, the m_B values and uncertainties from Table 3 are plotted. In the lower panel, m_B values have been corrected for host-galaxy $E(B\text{-}V)$ extinction. The error bars here are ~~much~~ uncertainty larger because the color excess must be multiplied by R_B in order to determine the resulting uncertainty on m_B.

[[This has already been said several times.]]

Figure 4 shows the measurement of $\Omega_{\rm M}$ and Ω_Λ resulting from the fits to the low-extinction primary subset (Subset 2); several parameters from these fits are tabulated in Fits 1–3 of Table 8. In Figure 4, the same low-redshift supernovae are inlcuded in all fits, but the high-redshfit sample is studied in various combinations. The filled contours show the combined limits using all of the

[[make this period a colon]]

[[Change this to Figures 10 and 4 (and then renumber them to be Figures 4 and 5, and of course shift the later figure numbers down one). In the following sentences, right here, describe Figure 10 and explain that Fit 3 is the primary fit of this paper. Also explain that all the other fits will be compared against it in what follows. So this is where we show the big result of this paper, right up front in the Results section.]]

Move the last column of this table to
become the second column of this table.

Table 8: Cosmological fits

Fit #	N_{SNe}	Min. χ^2	Ω_M for Flat[a]	Ω_Λ for Flat[a]	$\mathcal{M}$	α	High-Redshfit SNe Included in Fit[b]
			Primary				
Fits to Low-Extinction Subset (Subset 2)							
1	51	62	$0.22^{+0.07}_{0.07}$	$0.78^{+0.07}_{0.07}$	3.48 ± 0.05	1.52 ± 0.33	P99
2	32	38	$0.18^{+0.07}_{0.07}$	$0.82^{+0.07}_{0.07}$	3.47 ± 0.05	0.99 ± 0.34	New "HST" SNe from this paper
3	**61**	**76**	$\mathbf{0.21^{+0.06}_{0.05}}$	$\mathbf{0.79^{+0.05}_{0.06}}$	$\mathbf{3.47 \pm 0.05}$	$\mathbf{1.25 \pm 0.29}$	Primary Fit: **All SCP SNe**
Fits to Full Primary Subset (Subset 1), With Extinction Correction							
4	53	56	$0.19^{+0.20}_{0.16}$	$0.81^{+0.16}_{0.20}$	3.47 ± 0.06	1.19 ± 0.33	P99
5	34	44	$0.16^{+0.12}_{0.10}$	$0.84^{+0.10}_{0.12}$	3.47 ± 0.06	1.20 ± 0.32	New "HST" SNe from this paper
6	64	72	$0.18^{+0.11}_{0.10}$	$0.82^{+0.10}_{0.11}$	3.46 ± 0.06	1.07 ± 0.32	All SCP SNe.

a: This is the intersection of the fit probability distribution with the the line that assumes $\Omega_M + \Omega_\Lambda = 1$.
b: All fits include the low-redshift SNe from H96 and R99.

[[What happened to the other Hubble diagram figure with lots of SNe?]]

[[Make inner error bars wider than the outer error bars, so they can be seen for all these supernovae.]]

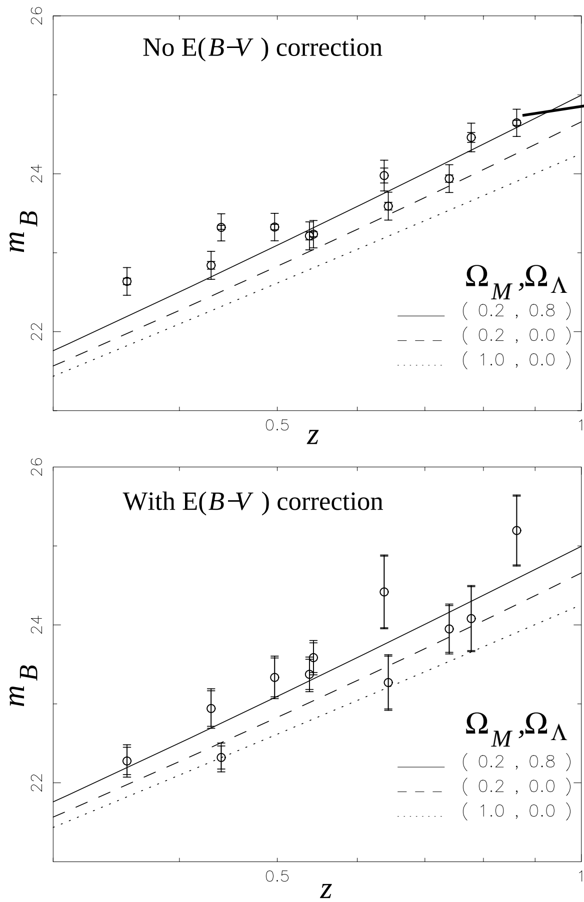

Fig. 3.— Hubble Diagram of effective m_B vs. redshift for the 11 SNe observed with WFPC2 and reported in this paper. In the upper plot, no host-galaxy $E(B\text{-}V)$ extinction corrections have been applied. Inner error bars only include the measurement error, and are generally a similar size to the plot symbols. Outer error bars include 0.17 magnitudes of intrinsic dispersion. In the lower plot, host-galaxy $E(B\text{-}V)$ extinction corrections have been applied; uncertainties have had $\delta E(B\text{-}V)\times R_B$ added in quadrature, where $\delta E(B\text{-}V)$ is the uncertainty in $E(B\text{-}V)$ and $R_B = 4.34$. Again, inner error bars represent only measurement uncertainties, while outer error bars include 0.11 magnitudes of intrinsic dispersion. Lines are for three different model cosmologies with the indicated values of Ω_M and Ω_Λ, ~~including the best fit flat universe case of $(\Omega_M, \Omega_\Lambda) = (0.2, 0.8)$~~.

Note that

SCP's high redshift supernovae, both from P99 and from this paper (Fit 3). The solid lines show confidence intervals from a fit using only the high-redshift SNe from this paper (Fit 2), and the dotted contours are from a fit using (only the P99 SNe (Fit 1). Fit 2 provides comparable and consistent limits on Ω_M and Ω_Λ to Fit 1 (which includes a greater number of high-redshift supernovae selected from P99).

~~Figure 5, and the bottom three lines of Table 8, show how the cosmological fits to the full primary subset (Subset 1) compare with host-galaxy extinction corrections applied.~~ The top row of fits from this figure are the same low-extinction subset fits plotted in Figure 4. The second row has $E(B\text{-}V)$ host-galaxy extinctions applied using the one-sided prior used by Fit E of P99 and Riess (1998) ~~and~~ discussed in § 3; because of bias introduced by this prior ~~(P99),~~ we do not recommend using these re- (P99). sults. The third row has full extinction corrections applied to supernova Subset 1, without any prior assumptions on the intrinsic $E(B\text{-}V)$ distribution. Two points are apparent from this plot. First, using a prior does, as expected, greatly reduce the apparent $E(B\text{-}V)$ error bars and hence apparently tightens the constraints of the cosmological confidence regions. However, this is a false impovement, since it comes at the cost of introducing a bias in the measurment. Second, the current set of supernovae provide much better limits on the cosmology than do the SNe Ia from previous high redshift samples when unbiased extinction corrections are applied. Whereas Figure 4 shows that the current set of supernovae give comparable limits on Ω_M and Ω_Λ when the low-extinction subsample is used with no host-galaxy extinction corrections, Figure 5 shows that the much higher precision color measurements from the WFPC2 data allows us directly to set much better limits on the effects of host-galaxy extinction on the cosmological results.

Figure 5 compares fits of the low-extinction samples to fits of the full samples with different approaches to extinction correction.

et al

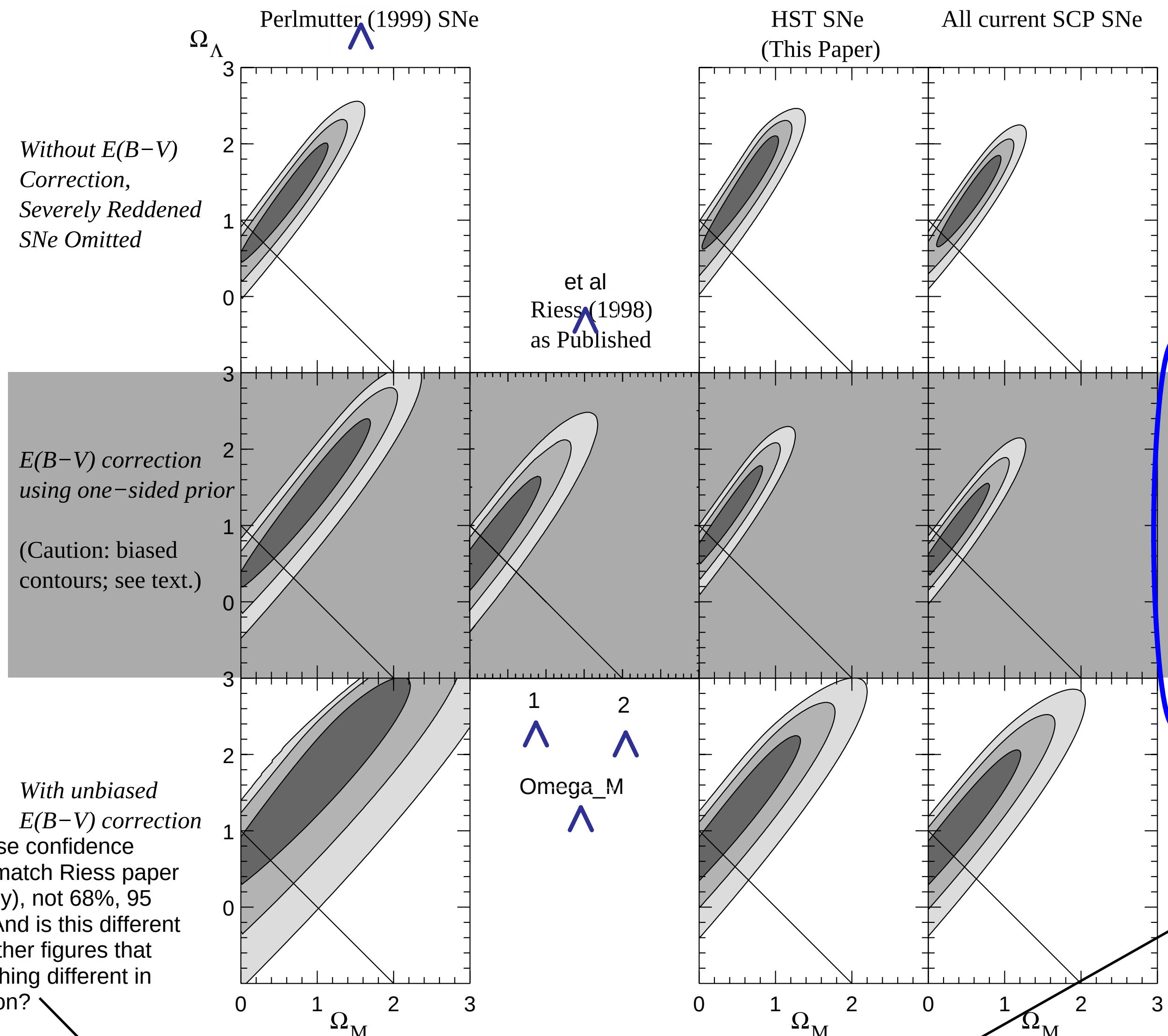

et al

Trim this extra gray background so that it doesn't extend past plots.

1

2

Omega_M

Really these confidence levels (to match Riess paper presumably), not 68%, 95 and 99? And is this different than the other figures that say something different in their caption?

to the low extinction primary subset (Subset 2),

Fig. 5.— 68.3%, 95.4%, and 99.7% confidence limits on Ω_M and Ω_Λ using different data subsets and methods for treating host-galaxy extinction corrections. The top row represents fits ~~from Subset 2,~~ where reddened supernovae have been omitted and host-galaxy extinction corrections are not applied. The second row shows fits where extinction corrections have been applied using a one-sided color excess prior ~~(see text); supernovae from Subset 1 went into these fits.~~ The third row shows fits with unbiased extinction corrections applied. Comparisons of the different subsets of data show that not only can the prior slightly bias the fit cosmology, but it also greatly reduces the effect of color errors on cosmology. The HST SNe presented in this paper show a marked improvement in the precision of the color measurements, and hence in the precision of the Ω_M and Ω_Λ measurements when a full extinction correction is applied.

to Subset 2

to the full primary subset (Subset 1),

Re-word so that this doesn't sound like such a good thing. (Maybe use some word like "apparently".)

This approach introduces bias and is not recommended (see text). [[Add another sentence here to explain that the Riess et al plot shown "as published" included two SNe from the SCP P99 sample, so is not completely independent. And either put back their dotted contours (and explain) or explain that they were taken out (since it is not exactly as published then).]]

[[Does Tonry et al do this kind of joint plot?]]

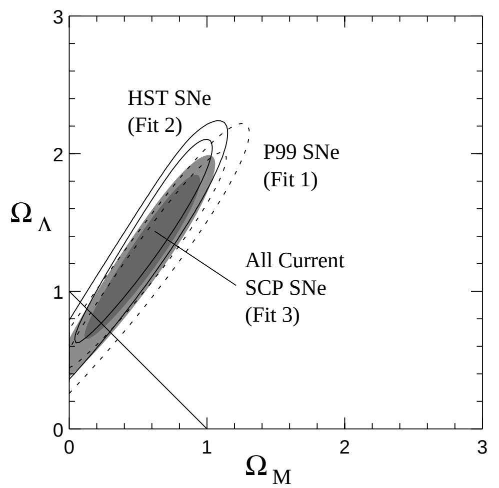

Put this at end of caption.

[[This caption still needs a little more re-wording to make sense.]]

Fig. 4.— New (HST) and old (P99) sets of high-redshift supernovae yield consistent measurements of Ω_M and Ω_Λ. Contours indicate the 68% and 90% confidence ~~intervals~~ regions for each fit. The dotted lines are contours ~~from Fit 1, using~~ are based on only high-redshift supernovae from P99 (Fit 1). The solid lines are contours ~~from Fit 2, using~~ based on only high-redshift supernovae from this paper (Fit 2). The filled contours combine all current high-redshift SCP supernovae.

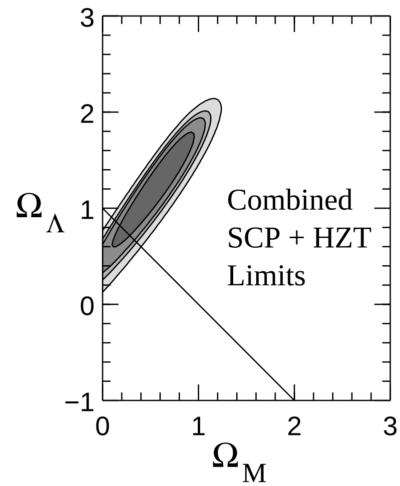

Fig. 6.— Ω_M and Ω_Λ 68%, 90%, 95%, and 99% confidence limits which combine the high-redshift data of the SCP (this paper, P99) and ~~the High-Z Team~~ (Riess 1998). The fit includes Subset 2 supernovae from the SCP plus the nine well-observed confirmed SNe Ia from Riess (1998). [[Explain here in caption, too, that this fit doesn't include SNe that Riess used from the SCP P99 data.]]

4.2. Combined High-Redshift Supernova Limits

Figure 6 shows the limits on Ω_M and Ω_Λ which combine the high-redshift supernova data of Riess (1998) together with the SCP data presented in this paper and in P99. The contours show confidence intervals from the 61 SNe of the low-extinction primary Subset 2 (used in Fit 3 of Table 8), plus the nine well-observed confirmed Type Ia supernovae from Riess (1998) (using their template fitting data); following the criteria of Subset 2, SN 1997ck has been omitted, as that supernova does not have a confirmed type identification nor a color measurement. We also omit from Riess et al (1998) the supernovae they measured using the "snapshot" method, and two SCP SNe ~~(already included in the P99 set)~~ that Riess et al used from the SCP P99 data set. This fit has a minimum χ^2 of 83 with 70 supernovae. Under the assumption of a flat universe, it yields a measurement of the mass density of $\Omega_M = 0.23 \pm 0.06$, or equivalently a cosmological constant of $\Omega_\Lambda = 0.77 \pm 0.06$. However, this fit should be approached with some caution, as the nine supernovae from the Riess (1998) team were not treated in exactly the same manner as the others. The details of the template fitting will naturally have been different, which can introduces small differences (see § 5.1). More importantly, the K-corrections applied by the Riess (1998) team to derive distance moduli were almost certainly different from those used in this paper. (The fact that many of their supernovae show significant negative values of $E(B\text{-}V)$ suggests that this effect may be non-negligible.)

because the uncertainties are much larger, and so these SNe don't contribute significantly?

Say why this error bar is worse than the one for our SNe alone, without the extra data? (Probably because its in a place on the paramter-space plane where magnitude contours get closer together so error bars get bigger.)

[[This doesn't seem consistant with the fact that the change in K-corrections shown in systematics section doesn't change cosmology fit much.]]

4.3. Dark Energy Equation of State

The fits of the previous section used a traditional Robertson-Walker cosmology where Ω_M is the energy density of non-relativistic matter (i.e. pressure $p = 0$), and Ω_Λ is the energy density in a cosmological constant (i.e. pressure $p = \quad \rho$, where ρ is the energy density). In Einstein's field equations, the gravitational effect enters in terms of

[[Explain that if it were not for Omega_m ~ 0.25 (with w = 0) then all you would need would be w < -1/3 to get acceleration, but because of this contribution to total w from Mass, you need dark energy to have w < -1/2.]]

$\rho+3p$. If $w \equiv p/\rho$ is the equation of state parameter, then for matter, $w = 0$ and for vacuum energy (i.e. a cosmological constant), $w = \ \ 1$. In fact, it is possible to achieve an accelerating Universe so long as there is a component with $w <\sim \ \ 1/2$. The Hubble diagram for high-redshift supernovae provide measurements of ~~limits on the value of~~ w (P99, Garnavich *et al.* 1998b). The top two panels of Figure 7 shows the joint confidence regions ~~limits~~ on $\Omega_{\rm M}$ and w for the SCP SNe, including the 11 new "HST" SNe, under the strongly-constraining assumption that w is constant, and that the Universe is flat, i.e. $\Omega_{\rm M} + \Omega_X = 1$ (where Ω_X is the energy density in the component with equation of state w, in units of the critical density). By themselves, the supernova data sets a limit of $w \lesssim \ \ 0.5$, for any positive value of $\Omega_{\rm M}$. However, w is not well bounded from below; although Figure 7 only shows confidence intervals down to $w = \ \ 2$, the 68% confidence interval from Fit 3 extends to $w < \ \ 5$, and the 99% confidence interval extends down to $w \sim \ \ 12$.

Other methods provide joint limits on $\Omega_{\rm M}$ and w which are complementary to the supernova limits. Two of these measurements are plotted in the middle row of Figure 7, compared with the supernova limits (in solid contours). In filled contours are limits on the $z \sim 0.15$ measurement of the two-point galaxy correlation function from the 2dF Galaxy Redshift Survey (2dFGRS) (Hawkins *et al.* 2002). This provides a measurement of $\Omega_{\rm M}(z)$ at $z = 0.15$; the the mild dependence of Omega_m on w ~~mild vairation of $\Omega_{\rm M}$ from w~~ comes from converting that measurement to a true $z = 0$ measurement of $\Omega_{\rm M}$. In dotted contours are limits based on the distance to the surface of last scattering at $z = 1089$ from the Wilkinson Microwave Anisotropy Probe (WMAP) (Bennett *et al.* 2003; Spergel *et al.* 2003). As both of these measurements show correlations between $\Omega_{\rm M}$ and w in a different sense from those of the supernova limits, the combined measurements provide much tighter overall limits on $\Omega_{\rm M}$. When the limits from the three data sets are combined, and the resulting probability distribution is marginalized over $\Omega_{\rm M}$, we measure a limit on w of $\ \ 1.15^{+0.17} \ \ 0.22$ (for the low-extinction subset), or $\ \ 1.17^{+0.22} \ \ 0.27$ (for the full primary subset with host-galaxy extinction corrections applied). These combined limits remain consistent with a low density universe dominated by a constant vacuum energy ($w = \ \ 1$), but also remain consistent with a very wide range of both constant-w and time-varying-w ~~other constat w~~ dark energy models.

[[This sentence still isn't very clear. Perhaps is should be explained a little more fully.]]

Fix the LaTeX

5. Systematic Errors

The effect of most systematic errors in the $\Omega_{\rm M}$ vs. Ω_Λ plane is asymmetric in a manner similar to the asymmetry of our statistical errors. For the effects listed below, a systematic difference will tend to move the confidence ellipses primarily along their major axis. In other words, for most systematic effects, we have a larger uncertainty in $\Omega_{\rm M} + \Omega_\Lambda$ than in $\Omega_{\rm M} \ \ \Omega_\Lambda$ (or, equivalently, in a measurement of $\Omega_{\rm M}$ or Ω_Λ alone under the assumption of a flat universe). This means that systematic effects do not currently seriously hamper the cosmological measurements from supernovae where they have the greatest weight, nor do they significantly diminish the direct evidence from supernovae for the presence of dark energy. However, they do limit the ability of supernovae to measure the spatial curvature ("geometry") of the Universe. (Note that the semi-major axis is not precisely in the direction of $\Omega_{\rm M} + \Omega_\Lambda$, nor is the semi-minor axis precisely aligned with $\Omega_{\rm M} \ \ \Omega_\Lambda$, but since these are useful constraints we will quantify the systematic uncertainties along these two directions.) Figure 5 Figure 8 shows the effects of some of the systematics discussed in the following subsections ~~below.~~

Systematic effects on flat-universe limits on w are relatively mild. The right column of Figure 5 Figure 8 shows the effect of the systematics on w versus Omega_m confidence regions ~~$\Omega_{\rm M}/w$ limits~~ derived from our supernova data alone. To quantify the effect of identfied systematics, in the following subsections, we identify the shift in the maximum-liklihood value of w when the supernova data is combined with the w versus Omega_m confidence regions ~~$\Omega_{\rm M}/w$ limits~~ from 2dFGRS and WMAP (See § 4.3.)

5.1. Fit Method

There are multiple reasonable choices for lightcurve fitting methods which yield slightly different results for the lightcurve parameters. For the supernovae in P99, the R-band data on high-redshift supernovae provided much stronger limits on the stretch (the shape of the lightcurve) than did more sparse I-band lightcurves. For consistency, the stretch values for the low redshift supernovae were therefore measured using only the B-band lightcurves in P99.

In this paper, there are high-quality photomet-

[[Is it possible to also say what the result is of a fit with no stretch correction (alpha = 0) like we did in P99?]]

Make the SN contours dotted, and the WMAP contours solid. Then label the WMAP contours with letters curving along the contour (and no arrow), Similarly label the 2dFGRS contours *on* the dark part of the contour at the top, and don't use an arrow.

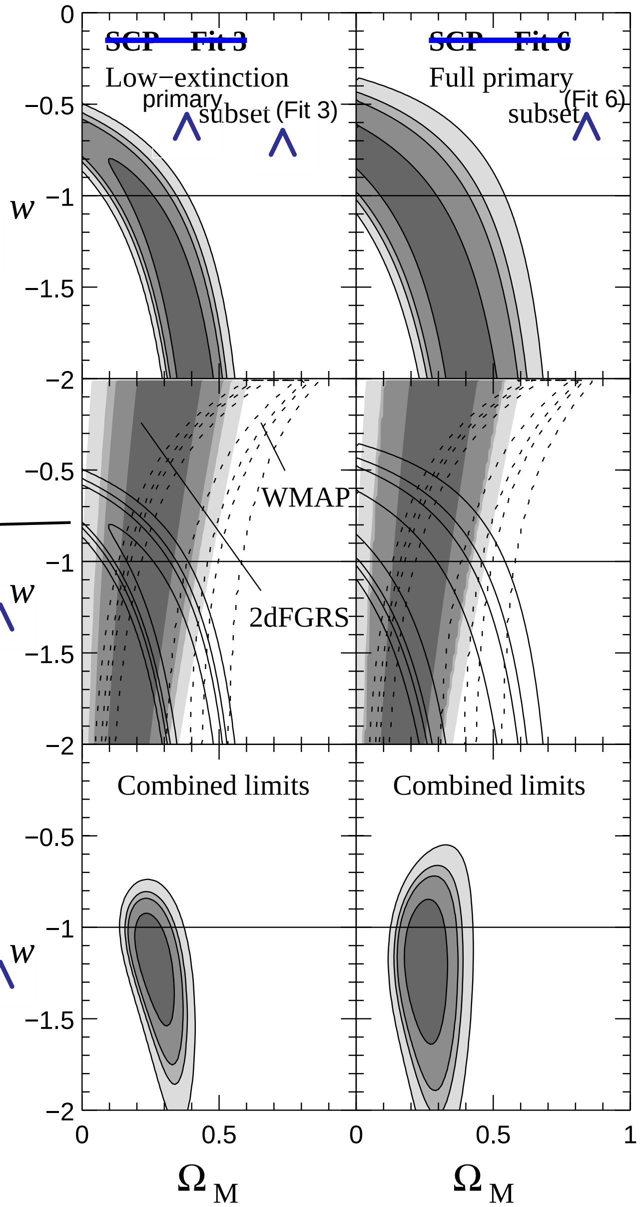

and that w is not time-varying.

Fig. 7.— Joint confidence limits on $\Omega_{\rm M}$ and w assuming $\Omega_{\rm M} + \Omega_X = 1$. Confidence limits plotted are 68%, 90%, 95%, and 99%. The left column shows fits to the low-extinction Subset 2; the right coumn shows fits to the full primary subset with unbiased individual host-galaxy extinction correctiones applied. The upper panels show the limits from the SCP supernovae alone. The middle panels overlay this (solid lines) with limits from 2dFGRS (filled contours) (Hawkins *et al.* 2002) and WMAP (dotted contours) (Bennett *et al.* 2003; Spergel *et al.* 2003). The bottom plot combines the three data sets to provide a combined limit on $\Omega_{\rm M}$ and w.

primary

Is there some way to word this so that it is clear that the contours represent the shifts if the systematic all went in one direction?

[[It might be better not to show this subplot (b), since most readers will think that the larger error contours represent how much systematic error is introduces with Host Galaxy extinction -- rather than just the difference of the center of the fit.]]

[[This last subplot (d) should be separate by some space (and maybe a title saying "For full extinction correction analyses") from the other 3.]]

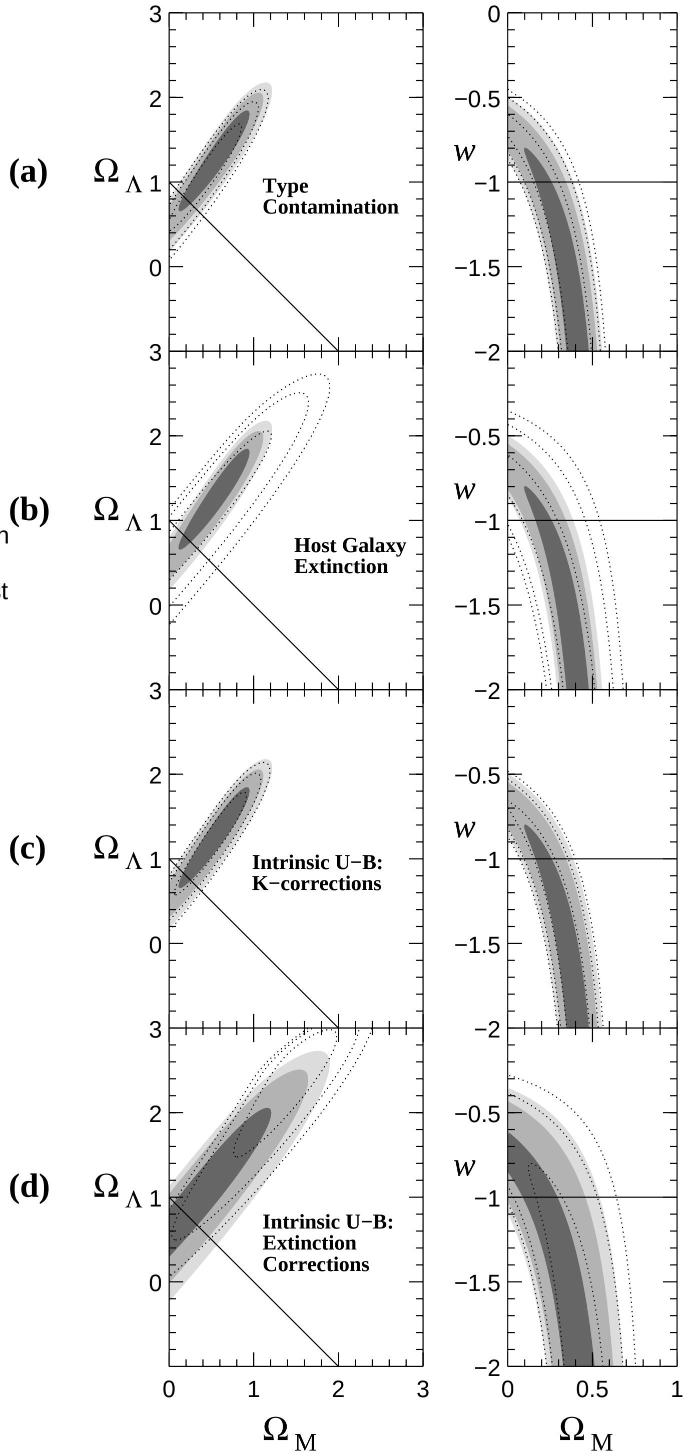

Fig. 8.— The effects of identified systematic errors on the cosmological parameters. The left column shows ~~fits to Ω_M and Ω_Λ;~~ and the right column ~~to Ω_M and the dark energy equation of state parameter w.~~ Rows (a)–(c) show our standard fit (Fit 3) in filled contours. (a) The dotted contours show the results of a fit to Subset 3, only those supernovae with the most secure spectral identifications as Type Ia SNe. (b) The dotted contours show the fit to Subset 1, with host-galaxy extinctions applied. (c) The dotted contorus show a fit to Subset 2, where K-corrections have been applied using a template spectum with an intrinsic value of U-B= 0.5 at the epoch of B-maximum. (d) The filled contours is Fit 6, our standard fit with host-galaxy extinction corrections applied; the dotted contours show a fit to the same Subset, but using a template spectrum with an intrinsic value of U-B= 0.5 for estimating both K-corrections and color excesses.

66%, 90%, and 99% confidence regions for Omega_Lambda versus Omega_M

the same confidence regions for a constant equation of state ratio, w, versus Omega_M.

ric measurements from WFPC2 in both R and I bands. Thus, data in both colors contributes significantly to the constraints on stretch. Additionally, the low background of the HST images, combined with the need to have previously subtracted the host galaxy background in order to combine HST and ground-based data, indicate that it is more appropriate to fit these supernovae with fixed rather than floating lightcurve zero offsets. As this is the most appropriate fit method for the HST data, the low redshift supernovae should be treated consistently. These procedures which are most appropriate for the HST supernovae were used for all new fits performed in this paper and listed in Tables 3 through 5.

To estimate the size of the effect due to these differences in fitting method, cosmological confidence intervals were generated from the "Case C" subset of P99 using the new fits presented in this paper and compared to the results quoted in P99 and other variations on the fitting method. Differences in the fit method can change the flat-universe value of Ω_M of $\sim$0.02, and the ~~minimum χ^2~~ value of $\Omega_M + \Omega_\Lambda$ by up to $\sim$0.8. (This is still well less than the major-axis extent of the statistical confidence ellipse in this direction.) We use these values as "fit-method" systematic uncertainties. We similarly performed joint fits to constant w versus Omega_m ~~Ω_M/w~~ in the flat-universe case to the supernovae from P99 with different lightcurve fit methodologices, and from these fits adopt a fit-method systematic uncertainty of 0.02 on constant w (once combined with limits from 2dFGRS and WMAP).

5.2. Supernova Type Contamination

All subsets of supernoave used for cosmological fits in this paper omit supernovae for which there is not a spectral confirmation of the supernova type. Nonetheless, it is possible in some cases where that confirmation is weak that we may have contimation from non-Type Ia supernovae. To estimate the effects of this, we performed fits using only those supernovae which have a firm indentification as Type Ia; this is Subset 3 from § 2.4. The comparison between our primary fit (Fit 3) and this fit with a more stringent type cut is shown in row (a) of Figure 5. This fit has a value of Ω_M in a flat universe which is 0.01 higher than that of Fit 3. The ~~minimum χ^2~~ value of $\Omega_M + \Omega_\Lambda$ is 0.28 magnitudes lower than that of Fit 3. We adopt these values as our "type contamination" systematic error.

The affect of changing our supernova subset on w is shown in the right panel of Figure 5a. Combined with the CMB and large scale structure mass measurement, the maximum likelihood value of w gets larger by 0.0; we adopt this as our type contamination systematic error on w.

5.3. Host-Galaxy Extinction

Figure 5b shows a direct comparison between the fits with and without extinction corrections applied. The filled contours do not have extinction corrections applied; they represent Fit 3, shown in Figure 4 and the left panel of Figure 7. The dotted contours do have extinction corrections applied; they represent Fit 6, shown in the lower right panel of Figure 5 and the right panel of Figure 7. Although the size of the confidence region obviously swells when $E(B\text{-}V)$ uncertainties are fully propogated into the cosmology, it is plain that the results with and without these corrections are consistent. The flat-universe values for these two fits are listed in Table 8, and differ by 0.03. The maximum likelihood value of $\Omega_M + \Omega_\Lambda$ differs by 0.44. Finally, the best-fit value of w when combined with 2dFGRS and WMAP changes by only 0.02 when individual host galaxy extinction corrections are applied. We adopt these values as the host-galaxy extinction systematic error for those fits where extinction corrections are not included as a part of the statistical error.

For the low-extinction primary subsample used for Fits 1-3, ~~Fit 1~~, we omitted supernovae which had both E(B-V) > 1 and ~~both~~ $E(B\text{-}V) > 3\sigma$, where σ represents just the measurement error, ~~and $E(B\text{-}V) > 0.1$,~~ to account for any intrinsic dispersion in $E(B\text{-}V)$. If, as mentioned in Section 3, our intrinsic B-V is ~ 0.02 magnitudes too blue, then three additional supernovae would have been omitted from our fits: two at low redshift, (SN 1992bh and SN 1993ag), and one from the set of HST-observed high-redshift SNe, (SN 1998as) Omitting these supernovae and repeating a fit without $E(B\text{-}V)$ corrections lowers the flat-unverse value of Ω_M by 0.03, and lowers the ~~minimum χ^2~~ value of $\Omega_M + \Omega_\Lambda$ by 0.18. As these values are equivalent to or lower than the host-galaxy extinction systematic errors derived from directly applying unbiased extinction corrections, we use the larger extinction systematic limits above for those fits where host-galaxy

[[Add parentheses.]]

Why not add this error in quadrature? It looks like it could be there at the same time as the bigger one.

Refine this point, and make it based on arguments of continuity with the lower redshift SNe.

extinction is not directly treated as a statistical error.

5.4. K-corrections and Supernova Colors

The generation of the spectral template used for calculating K-corrections is described in § 2.3. The degree to which uncertainties in the K-correction introduce systematic uncertainties into the cosmological parameters depends on whether or not extinction corrections are being individually applied to supernovae. In particular, our K-corrections are most uncertain in the rest-frame U-band range of the supernova spectrum, due to limited published spectrophotmetry. As discussed in § 2.2, our primary fits use a spectral template which has a color U-B= 0.4 at the epoch of B-maximum. We have investigated the effects on our cosmology of replacing the spectral templated used both for K-corrections and for determining color excesses with a template that has U-B= 0.5 at the epoch of maximum B light.

Figure 5c shows affect on the fitted cosmology caused by using the different template for calculating K-corrections when individual host-galaxy extinction corrections are not applied. These effects are very mild, indicating that our K-corrections are robust with respect to the intrinsic U-B color of a supernova. Based on the comparison of these fits, we adopt a K-correcton systematic uncertainty of 0.01 on $\Omega_{\rm M}$ in a flat universe, 0.13 on $\Omega_{\rm M}+\Omega_\Lambda$, and 0.10 in w.

Although the effects of a different intrinsic U-B color on the K-corrections are mild, the effects on calculated color excesses are much greater. Figure 5d shows the difference between Fit 6, where host-galaxy extinction corrections have been applied using our standard color-excess values, and a fit where color-excess values have been determined assuming the intrinsic U-B color of a supernova is 0.5 at maximum light. As with all other systematics, the primary effect is to move the confidence intervals along their major axis. In this case, the large shift in $\Omega_{\rm M}+\Omega_\Lambda$ is mainly due to the fact that with this bluer assumption amout U-B, we would believe that all of our $z > 0.7$ supernovae are suffering from a significant about of host-galaxy extinction, and as such all need to be dereddened. Given that the more distant supernovae are dimmer and thus closer to our detection limits than the moderate redshift supernovae, this scenario is implausible. If anything, one would expect the higher redshift supernovae to be *less* subject to host-galaxy extinction due to selection effects. Nonetheless, a value of U-B= 0.5 at the epoch of B-band maximum is currently plausible given the U-band information available. Only for those fits where extinction corrections are applied, we have an additional intrinsic U-B systematic error of 0.06 on the flat-universe value of $\Omega_{\rm M}$, and a systematic error of 2.5 on $\Omega_{\rm M}+\Omega_\Lambda$. That it is implausible that our highest redshift supernovae are the most extinguished makes it likely that this is an overestimate of this systematic.

The systematic effect of changing the assumed intrinsic color is much less ~~not as~~ significant on the flat-universe value of w a constant w. ~~as it is on the $w=0$ value of $\Omega_{\rm M}+\Omega_\Lambda$~~. When combined with the CMB/large scale structure mass measurement, the best-fit value of w is only 0.05 higher than the value from our primary extinction-corrected fit. We adopt this difference as our systematic uncertainty on w when host-galaxy extinction corrections are applied.

5.5. Malmquist Bias

As most of our supernovae are from flux-limited samples, they will suffer Malmquist bias (Malmquist 1924, 1936). This effect was discussed extensively in P99, and here we update that discussion to include our new HST SNe Ia. For the measurement of the cosmological parameters, it is the difference between the Malmquist bias of the low-redshift and high-redshift samples which matters. In particular, the probability of $\Omega_\Lambda > 0$ is enhanced only if the low-redshift SNe suffer more Malmquist bias than the high-redshift SNe, as this makes the high-redshift SNe Ia seem fainter.

The P99 high-redshift dataset was estimated to have little Malmquist bias (0.01 mag) because the SN discovery magnitudes were decorrelated with the measured peak magnitudes. However, for the new HST sample, nine of the eleven SNe Ia selected from full search samples were found almost exactly at maximum light. This may reflect a spectroscopic flux limit superimposed on the original search flux limit since only spectroscopically confirmed SNe Ia were considered, and of those, generally the higher redshift SNe Ia from a given search were chosen, for HST for follow-up. In particular, the SNe Ia selected for follow-up from the